



Deposited via The University of Leeds.

White Rose Research Online URL for this paper:

<https://eprints.whiterose.ac.uk/id/eprint/80225/>

Version: Accepted Version

Article:

Ivanovic, RF, Valdes, PJ, Gregoire, LJ et al. (2013) Sensitivity of modern climate to the presence, strength and salinity of Mediterranean-Atlantic exchange in a global General Circulation Model. *Climate Dynamics: observational, theoretical and computational research on the climate system*, 42 (3-4). 859 - 877. ISSN: 0930-7575

<https://doi.org/10.1007/s00382-013-1680-5>

Reuse

Items deposited in White Rose Research Online are protected by copyright, with all rights reserved unless indicated otherwise. They may be downloaded and/or printed for private study, or other acts as permitted by national copyright laws. The publisher or other rights holders may allow further reproduction and re-use of the full text version. This is indicated by the licence information on the White Rose Research Online record for the item.

Takedown

If you consider content in White Rose Research Online to be in breach of UK law, please notify us by emailing eprints@whiterose.ac.uk including the URL of the record and the reason for the withdrawal request.

1 **Sensitivity of modern climate to the presence, strength and salinity of Mediterranean-**
2 **Atlantic exchange in a global General Circulation Model.**

3

4 **Authors and affiliations**

5 Ruza F. Ivanovic^{1*}, Paul J. Valdes¹, Lauren Gregoire¹, Rachel Flecker¹ and Marcus Gutjahr²

6

7 ¹School of Geographical Sciences, University of Bristol, University Road, Bristol, BS8 2YF,
8 UK.

9 ²Ocean and Earth Sciences, National Oceanography Centre, University of Southampton
10 Waterfront Campus, European Way, Southampton, SO 14 3ZH, UK.

11

12 * Corresponding author email: Ruza.Ivanovic@bristol.ac.uk, Tel.: +44 (0)117 331 7313, Fax:
13 +44 (0)117 928 7878

14

15 **Keywords**

16 Mediterranean Outflow Water; Mediterranean salinity; North Atlantic circulation; North
17 Atlantic climate; Atlantic Meridional Ocean Circulation (AMOC); North Atlantic Deep
18 Water (NADW)

19

20 **Abstract**

21 Mediterranean Outflow Water (MOW) is thought to be a key contributor to the strength and
22 stability of Atlantic Meridional Overturning Circulation (AMOC), but the future of
23 Mediterranean-Atlantic water exchange is uncertain. It is chiefly dependent on the difference
24 between Mediterranean and Atlantic temperature and salinity characteristics, and as a semi-
25 enclosed basin, the Mediterranean is particularly vulnerable to future changes in climate and
26 water usage. Certainly, there is strong geologic evidence that the Mediterranean underwent
27 dramatic salinity and sea-level fluctuations in the past.

28 Here, we use a fully coupled atmosphere-ocean General Circulation Model to examine the
29 impact of changes in Mediterranean-Atlantic exchange on global ocean circulation and
30 climate. Our results suggest that MOW strengthens and possibly stabilises the AMOC not
31 through any contribution towards NADW formation, but by delivering relatively warm,
32 saline water to southbound Atlantic currents below 800 m. However, we find almost no
33 climate signal associated with changes in Mediterranean-Atlantic flow strength.

34 Mediterranean salinity, on the other hand, controls MOW buoyancy in the Atlantic and
35 therefore affects its interaction with the shallow-intermediate circulation patterns that govern
36 surface climate. Changing Mediterranean salinity by a factor of two reorganises shallow
37 North Atlantic circulation, resulting in regional climate anomalies in the North Atlantic,
38 Labrador and Greenland-Iceland-Norwegian Seas of ± 4 °C or more. Although such major
39 variations in salinity are believed to have occurred in the past, they are unlikely to occur in
40 the near future. However, our work does suggest that changes in the Mediterranean's
41 hydrological balance can impact global-scale climate.

42

43

44 **1. Introduction**

45 The exchange of water between the Mediterranean and Atlantic, which today occurs through
46 the Gibraltar Straits, is an important control on Mediterranean water temperature and salinity
47 characteristics (Béthoux and Pierre 1999; Bethoux and Gentili 1999; Bethoux et al. 1999;
48 Cacho et al. 2002; Gómez 2003; Dubois et al. 2011). These in turn affect thermohaline ocean
49 circulation in the Mediterranean basin, redistributing heat and impacting regional climate
50 (Candela 1991; Alhammoud et al. 2010; Sanchez-Gomez et al. 2011). But far from being
51 unilateral, the system feeds back into itself. The geometry of the Gibraltar Straits; which is
52 influenced by processes of erosion, tectonics and changes in eustatic sea level (Bethoux and
53 Gentili 1999; Loget and Vandendriessche 2006; Govers et al. 2009; Alhammoud et al. 2010);
54 governs the volume of water that can physically pass between basins at any one time and so
55 can be described as the primary control on Mediterranean-Atlantic exchange (e.g. Stommel
56 and Farmer 1952, 1953; Bryden and Kinder 1991; Bryden et al. 1994; Rogerson et al. 2012).
57 However, salinity and temperature exchange through the Straits is also regulated by the
58 density gradient across it (e.g. Bryden et al. 1994; Thorpe and Bigg 2000; Mariotti et al.
59 2002; Somot et al. 2006), therefore providing a feedback system between Mediterranean
60 water characteristics and Mediterranean-Atlantic exchange.

61 A local surfeit in evaporation over precipitation and runoff causes a freshwater deficit in
62 the Mediterranean of $400\text{-}600\text{ mm yr}^{-1}$ (Bryden et al. 1994; Bethoux and Gentili 1999;
63 Jungclaus and Mellor 2000; Tsimplis and Bryden 2000; Mariotti et al. 2002; Gómez 2003)
64 and is responsible for a salinity difference of 2-3 psu between the westernmost Mediterranean
65 and eastern North Atlantic (Boyer et al. 2009). This salinity difference dominates the density
66 gradient across the Gibraltar Straits and so influences Mediterranean-Atlantic exchange,
67 which acts to equalise conditions in the two basins (Bryden et al. 1994; Jungclaus and Mellor
68 2000). Thus, by affecting local water temperature and salinity properties, regional changes in

69 Mediterranean climate and circulation contribute towards the strength of Mediterranean-
70 Atlantic exchange (e.g. Bethoux and Gentili 1999; Mariotti et al. 2002).

71 Interestingly, both model and observational data suggest that due to regional climate
72 warming and the diversion of fluvial runoff for domestic and agricultural purposes, the
73 Mediterranean freshwater deficit has increased by over 10 % in the last 40-50 years, affecting
74 local climate and Mediterranean deep water formation (Bethoux et al. 1999; Mariotti et al.
75 2002; Skliris and Lascaratos 2004; Xoplaki et al. 2006; Dietrich et al. 2008; Vargas-Yáñez et
76 al. 2010). This trend is expected to persist, possibly increasing towards the end of the 21st
77 Century (Somot et al. 2006, 2008; Christensen and Christensen 2007; Gao and Giorgi 2008;
78 Giorgi and Lionello 2008; Mariotti et al. 2008; Dubois et al. 2011; García-Ruiz et al. 2011;
79 Sanchez-Gomez et al. 2011), implying that changes in Mediterranean-Atlantic flow strength
80 are already afoot and may accelerate.

81 Further to its influence on the climate and thermohaline circulation of the Mediterranean,
82 flow through the Gibraltar Straits has wider, global significance through its effect on North
83 Atlantic Ocean circulation. For example, it has long been supposed that Mediterranean
84 Outflow Water (MOW) contributes towards the pattern and vigour of the Atlantic Meridional
85 Overturning Circulation (AMOC). The earliest hypotheses (Reid 1978, 1979) suggested that
86 upon leaving the Gibraltar Straits, a core of MOW takes a direct, northward flow path to the
87 northernmost North Atlantic and Greenland-Iceland-Norwegian (GIN) Seas, thus providing
88 relatively saline waters to areas of deep water formation. It was proposed that upon cooling,
89 the relatively high-salinity, MOW-origin waters contribute towards destabilising the water
90 column and thus drive local overturning. However, this *deep source* hypothesis, so termed by
91 McCartney and Mauritzen (2001), has for the most part been disproved by more recent ocean
92 model investigations (e.g. Stanev 1992; Mauritzen et al. 2001; New et al. 2001) and
93 observational data (e.g. McCartney and Mauritzen 2001; Bower et al. 2002a, 2002b). These

94 newer studies favour a *shallow source* hypothesis (McCartney and Mauritzen 2001),
95 suggesting that MOW spreads predominantly westwards to precondition the north-eastward
96 flowing North Atlantic Current with relatively warm, saline waters. These waters are thus
97 transported to the northernmost North Atlantic and GIN Seas, providing an indirect, but
98 nevertheless important, source of warm, saline waters to the high latitude sites of NADW
99 formation.

100 It should be noted that although perhaps more famous for his *deep source* hypothesis,
101 Reid himself also viewed the westward flow path as the ‘most obvious’ and well documented
102 route of MOW to the North Atlantic, commenting that subsequent mixing with intermediate
103 North Atlantic Central Waters supplies relatively warm, high salinity water to the high
104 latitudes (Reid 1978, 1979). Certainly the global General Circulation Models (GCMs)
105 hitherto used to investigate MOW generally agree on its mainly westward flow into the North
106 Atlantic at depth (Rahmstorf 1998; Bigg and Wadley 2001; Chan and Motoi 2003; Rogerson
107 et al. 2010), broadly emulating the observed spread of relatively warm, saline,
108 Mediterranean-origin water in modern North Atlantic Central Waters (Boyer et al. 2009).

109 Thus it would seem that questions over MOW’s flow path in the North Atlantic and
110 transportation to the GIN Seas are largely resolved. Yet, uncertainty remains over the extent
111 to which MOW is capable of influencing North Atlantic circulation and global climate. For
112 example, there is strong model-based (Bigg and Wadley 2001; Rogerson et al. 2010) and
113 proxy-based (including Rogerson et al. 2006, 2010; Voelker et al. 2006; Penaud et al. 2011)
114 evidence to suggest that for cold periods in the recent geologic past (50 ka to present),
115 strengthened Mediterranean-Atlantic exchange (and hence enhanced MOW) provided a
116 crucial negative feedback to North Atlantic freshening, boosting NADW formation during
117 intervals of weaker or interrupted Atlantic thermohaline circulation. Penaud et al. (2011) even

118 propose that MOW could be the trigger for switching between stadial and interstadial AMOC
119 modes.

120 Similarly, others have speculated that anthropogenic influences on the Mediterranean are
121 affecting AMOC strength in the present day and will continue to do so in the coming decades
122 and centuries. For example, Johnson (1997) proposed that recent and near-future
123 amplification of the Mediterranean freshwater deficit (e.g. Somot et al. 2006; Dietrich et al.
124 2008; Mariotti 2010; Vargas-Yáñez et al. 2010) will raise the Mediterranean-Atlantic density
125 gradient enough to fully deflect the Gulf Stream and thus induce Northern Hemisphere
126 Glaciation. In an equally speculative claim, Gómez (2003) suggested that future
127 Mediterranean climatic changes or outright damming of the Gibraltar Straits (as advised by
128 Johnson 1997) would reduce AMOC strength and stability; a sentiment echoed by Bethoux et
129 al. (1999) who suggest that without MOW, NADW formation could not be continuous
130 throughout the year. To test the hypothesis put forward by Johnson (1997), Rahmstorf (1998)
131 investigated the impact of human-induced changes in Mediterranean salinity on North
132 Atlantic circulation and climate. Coupling his ocean GCM to a simple atmospheric energy
133 balance model in this study, Rahmstorf concludes that the enhanced freshwater-deficit, hailed
134 by Johnson (1997) as the bringer of the next Ice Age, has negligible impact on North Atlantic
135 circulation and hence negligible impact on climate; the increase in Mediterranean salinity and
136 MOW flow strength is simply too small and MOW is unable to bring about Northern
137 Hemisphere Glaciation.

138 On the other hand, both Rahmstorf (1998) and Chan and Motoi (2003) suggest that MOW
139 contributes 1-2 Sv of flow to the present day AMOC south of the Gibraltar Straits, although it
140 has no direct impact on the overall maximum overturning strength. This is also seen in the
141 ocean modelling study carried out by Kahana (2005). These GCM findings do, to some
142 extent, support the postulations of Bethoux et al. (1999) and Gómez (2003) and furthermore,

143 they show a small climatic signal associated with the existence of MOW in the North
144 Atlantic. For example, Rahmstorf (1998) finds that the presence of MOW enhances the Gulf
145 Stream, which warms the surface North Atlantic by up to 0.3 °C, whilst Chan and Motoi
146 (2003) show that removing MOW for a period of several centuries, reduces meridional
147 overturning in Antarctic Bottom Water formation and cools Southern Ocean air temperatures
148 by up to 6 °C.

149 However, beyond blocking Mediterranean-Atlantic exchange (Rahmstorf 1998; Chan and
150 Motoi 2003), perturbations to modern MOW strength and salinity in global GCM studies
151 have so far been small (Rahmstorf 1998). So the question remains; how much influence is
152 MOW actually able to exert over global ocean circulation and climate? To address this, we
153 performed a series of idealised simulations of extreme changes in Mediterranean-Atlantic
154 exchange strength and salinity. These were run using a fully-coupled atmosphere-ocean GCM
155 (HadCM3), which, although no longer considered state-of-the-art, enables the simulations to
156 be integrated over a period of several centuries. According to the only other published
157 atmosphere-ocean GCM studies of MOW's impact on global ocean circulation and climate,
158 this is necessary in order to fully capture the climate signal associated with changes in MOW
159 (Chan and Motoi 2003) and to enable the model to reach a near steady state (Ivanovic et al.
160 2013). Thus, as well as emulating the standard 'on/off' GCM experiment performed by
161 Rahmstorf (1998) and Chan and Motoi (2003), we were able to test more rigorously the
162 ability of MOW to impact modern North Atlantic circulation and global climate.

163

164 **2. Methods**

165 In this section we briefly describe the global GCM used for this investigation, giving specific
166 details about how the model simulates Mediterranean-Atlantic exchange. Following this, we
167 outline the three experiments used to test the impact of (i) the presence, (ii) the strength and

168 (iii) the salinity of Mediterranean-Atlantic exchange on modelled ocean circulation and
169 climate.

170

171 **2.1. Model Description**

172 For this study, we used version 4.5 of the UK Met Office's fully coupled atmosphere-ocean
173 GCM HadCM3. The atmosphere model has a horizontal resolution of $2.5^\circ \times 3.75^\circ$, 19
174 vertical layers based on a hybrid vertical coordinate scheme (Simmons and Burridge 1981)
175 and a timestep of 30 minutes. The model includes physical parameterisations for the radiation
176 scheme (Edwards and Slingo 1996), convection scheme (Gregory et al. 1997) and land
177 surface scheme (MOSES-1; Cox et al. 1999). The ocean model grid has half the temporal
178 resolution of the atmosphere model, with a timestep of one hour, but is more finely resolved.
179 It has a horizontal resolution of $1.25^\circ \times 1.25^\circ$ and 20 vertical levels that are distributed on a
180 depth based (z) coordinate system, as given by Table 2 in Johns et al. (1997), to give
181 maximum resolution towards the ocean surface. Level spacing is small (10 m) near the
182 surface to resolve the mixed layer, but increases with depth, reaching 615 m for levels below
183 1193 m deep.

184 The ocean model's physical parameterisations include the eddy-mixing scheme of
185 Visbeck et al. (1997), the isopycnal diffusion scheme of Gent and McWilliams (1990) and a
186 simple thermodynamic sea ice scheme for ice concentration (Hibler 1979) and ice leads and
187 drift (Cattle et al. 1995). Gordon et al. (2000) show that the model adequately reproduces
188 modern sea surface temperatures without the need for unphysical 'flux adjustments' at the
189 ocean-atmosphere interface. The ocean component of HadCM3 has a fixed lid; in other
190 words, the volume of the ocean grid boxes (and hence sea level) cannot vary. Evaporation,
191 precipitation and river runoff are therefore represented as a salt flux (Gordon et al. 2000).

192 Once per model-day, the atmosphere and ocean components pass across the fluxes
193 accumulated over the previous 24 model-hours. To accommodate the different horizontal
194 resolutions, the ocean grid is aligned with the atmosphere grid and the data is respectively
195 averaged and interpolated during the coupling. River discharge is implicitly simulated using
196 grid-defined river catchments and estuaries, which instantaneously deliver continental runoff
197 to the coasts. For more details on the model and its constituent components, including
198 improvements on earlier versions, see Gordon et al. (2000) and Pope et al. (2000).

199

200 **2.2. Mediterranean-Atlantic exchange**

201 Due to the restrictions of global GCM grid resolution, it is a challenge to represent shallow,
202 narrow marine gateways such as the Gibraltar Straits, which is as shallow as 300 m and as
203 narrow as 14 km (Candela 1991; Gómez 2003). Mediterranean-Atlantic exchange can be (and
204 in many cases is) simply prescribed as a boundary condition to the North Atlantic ocean, but
205 this allows for neither a full mechanistic investigation of the dynamical responses and
206 feedbacks to changes in global or regional climates, nor a thorough examination of the
207 response to forcings originating in the Mediterranean Sea or North Atlantic Ocean. To do this
208 in global GCMs, there are two approaches for modelling the exchange. The first is to use an
209 unrealistically wide and deep *open seaway* to connect the two basins. This is the approach
210 adopted by Bigg and Wadley (2001) and Rogerson et al. (2010) to investigate the effect of
211 changing North Atlantic circulation and water-column characteristics on the intensity of
212 Mediterranean-Atlantic exchange, and the resulting feedback to North Atlantic salinity,
213 temperature and circulation patterns. It is worth noting that in both of these cases, a realistic
214 rate of exchange (1 Sv) is achieved, despite the oversized seaway.

215 The second approach is to have a land bridge connecting North Africa (Morocco) with
216 Southern Spain in the model and use a physical parameterisation of the net flows, which we

217 will refer to as a *pipe*. This parameterisation mixes thermal and haline properties across the
218 Gibraltar Straits and in this way emulates the exchange that is achieved with open flow
219 through the narrow, shallow Straits in reality. For example, in their studies of the impact of
220 changing Mediterranean-Atlantic exchange properties on Atlantic circulation and global
221 climate, Rahmstorf (1998) and Chan and Motoi (2003) replace water column temperature and
222 salinity properties in the upper 600 m of the two grid boxes situated either side of their
223 Morocco-Spain land bridge with the mean values for the pair at every time-step, resulting in
224 complete mixing across the Straits.

225 HadCM3 employs a version of the latter of these two methods, using a *pipe* to exchange
226 water across the land bridge connecting Morocco and Spain. The parameterisation, described
227 in more detail below, achieves partial mixing across the Straits according to a coefficient of
228 mixing (μ) as well as the comparative characteristics of the Alboran Sea (in the westernmost
229 Mediterranean) and the Gulf of Cadiz (in the North Atlantic), which is more realistic than
230 total mixing. This mixing takes place between the temperature and salinity tracer fields across
231 two pairs of grid boxes situated immediately adjacent to the land bridge; one pair in the
232 Alboran Sea and one pair in the Mediterranean. The depth of the *pipe* is constrained by the
233 minimum bathymetry of any one of these boxes, which is ~ 1 km, 13 vertical levels. For
234 every level and at every timestep, the mean of the four points is calculated for each tracer
235 field (\bar{T}). Then, where (T_j) is the tracer for each of the four grid boxes, the difference
236 between the old (previous timestep) and the new (current timestep) tracer is given as:

$$237 \left. \frac{\partial T_j}{\partial t} \right|_{pipe} = \mu(T_j - \bar{T})$$

238 (Gordon et al. 2000), where $\left. \frac{\partial T_j}{\partial t} \right|_{pipe}$ is the tracer tendency for the *pipe* parameterisation.

239 Thus, the model exchanges temperature and salinity properties based on the temperature and
240 salinity gradients existing at every ocean level and at every timestep of the model run. The
241 constant μ (set at $9.6e^{-5}$) defines the coefficient of mixing; that is, the proportion of each grid-
242 box that will be mixed, thus representing the control of Straits geometry on the exchange.
243 There is no advection of water through the *pipe*. However, the parameterised exchange in
244 temperature and salinity leads to flow in and out of boxes on either side of the *pipe*. The
245 water and salinity fluxes in and out of the Mediterranean Sea presented in this study were
246 calculated in the westernmost grid boxes of the Straits, immediately adjacent to the Morocco-
247 Spain land bridge. The mixing constant μ has been set to achieve 1 Sv of transport between
248 the Mediterranean and Atlantic in each direction, which is close to observational values
249 ($>0.74 \pm 0.05$ Sv; García-Lafuente et al. 2011). Although the geometry of the *pipe* remains
250 constrained by the ocean model's resolution, a more realistic rate of flow can be achieved
251 than by having a similarly size-constrained *open seaway* (as in Ivanovic et al. 2013).
252 Therefore, we chose to use this *pipe* set up in the experiments presented here.

253 Even though the modern Gibraltar Straits is only 300 m deep, MOW is observed to
254 rapidly descend the continental slope and settle at around 1000 m by 8.75° W in the modern
255 ocean, from where it spreads westwards into the North Atlantic (e.g. Baringer and Price
256 1999; Serra et al. 2005; Dietrich et al. 2008; Boyer et al. 2009). Because of the width of the
257 Morocco-Spain land bridge in HadCM3, which is constrained by horizontal grid resolution,
258 this makes 1000 m an appropriate depth for the *pipe* configuration, enabling the model to
259 simulate the large scale features of MOW's flow path in the North Atlantic. The resulting
260 eastward surface flow of North Atlantic Central Water into the Mediterranean and a deeper
261 westward flow of Mediterranean Outflow Water (MOW) into the Atlantic matches the

262 observed two-layer flow structure for flow through the Gibraltar Straits. The interface,
263 defined as the ‘depth of maximum vertical shear’ (Tsimplis and Bryden 2000), lies roughly
264 halfway between the surface and sill depth; at around 500 m in HadCM3, where the sill depth
265 is 1000 m (this study), and around 150 m in observations for a sill depth of 300 m (Bethoux
266 and Gentili 1999; Tsimplis and Bryden 2000; Gómez 2003; Boyer et al. 2009).

267 HadCM3 is not spatially fine-scaled enough to accurately resolve MOW eddies (*meddies*)
268 or its two-core flow structure observed for the narrow eastern boundary current (e.g.
269 Jungclaus and Mellor 2000; Johnson et al. 2002; Papadakis et al. 2003; Serra et al. 2005). The
270 model therefore probably underestimates shallow-intermediate level mixing of MOW and
271 Atlantic water in the eastern Atlantic. For example, results presented by Ivanovic et al. (2013)
272 suggest that increased mixing of Mediterranean and Atlantic water in the Gibraltar Strait-Gulf
273 of Cadiz region does slightly improve the HadCM3 representation of the MOW plume in the
274 modern North Atlantic. Similarly, our study is limited by its use of a depth based vertical
275 coordinate system (Johns et al. 1997), which incompletely resolves the dense overflow of
276 MOW from the Gibraltar Straits sill. As a result, the model has a tendency to overestimate the
277 mixing of MOW with surrounding water, simulating North Atlantic entrainment, as it
278 descends the continental shelf. These two limitations may affect the model’s sensitivity to
279 changes in MOW density, perhaps under-projecting any buoyancy anomalies; a caveat that
280 should be considered when interpreting the results of any such change. However, these
281 effects also partly counteract each other. Thus overall, the model’s ability to simulate the
282 large-scale features of MOW in the North Atlantic (e.g. as seen in Boyer et al. 2009) makes
283 the standard *pipe* set-up in HadCM3 an appropriate *control* configuration for this
284 investigation.

285 Due to the Mediterranean’s net annual evaporation from the basin (e.g. Bethoux and
286 Gentili 1999; Mariotti et al. 2002), there is a net transport from the Atlantic to the

287 Mediterranean. To conserve salinity in a steady state Mediterranean there is no net export of
288 salt through the Gibraltar Straits. In our fixed-lid model, however, net evaporation from the
289 Mediterranean Sea is represented as a salt flux rather than a true freshwater flux; there is no
290 net water flux across the Gibraltar Strait, but there is a net salt flux across it. This export of
291 salt from the Mediterranean has the same significance as the outflow salinity transport
292 defined by Bryden et al. (1994) as the outflow transport of MOW multiplied by the salinity
293 excess carried by the MOW over the incoming Atlantic water. The *pipe* parameterisation in
294 our model only allows a mean salt export of around 0.6 psu Sv, less than half of the outflow
295 salinity transport of ~ 1.5 psu Sv (Bryden et al. 1994). Moreover, this salinity flux is
296 controlled by the parameter μ and in the *control* simulation, the *pipe* does not conserve salt in
297 the Mediterranean Sea, which has a drift of 9.0×10^{-4} psu yr⁻¹. This drift is equivalent to
298 observations of increased Mediterranean salinity by 8.0 - 9.2×10^{-4} psu yr⁻¹ over the past 50
299 years (e.g. Dietrich et al. 2008; Vargas-Yáñez et al. 2010); a rate that is projected to nearly
300 triple by 2100 (Somot et al. 2006).

301 MOW's influence on the HadCM3 North Atlantic were identified by comparing our
302 *control* climate to a simulation which has no Mediterranean-Atlantic exchange; see section
303 2.3, experiment (a). Consequently, we can see that in both the *control* simulation (Fig. 1) and
304 modern observations (e.g. Boyer et al. 2009), MOW constitutes a distinct plume of relatively
305 warm (up to +6 °C) and highly saline (up to +1.8 psu) water protruding into North Atlantic
306 Central Waters, where it spreads predominantly westwards and mixes with surrounding
307 intermediate waters. In the modern North Atlantic, the MOW plume is centred at 1000-1200
308 m below the ocean surface (Boyer et al. 2009), whereas in HadCM3, the plume lies a little
309 deeper at 1200-1500 m (Fig. 1). Opening the Gibraltar Straits seaway in the model, rather
310 than using a *pipe*, does cause a shoaling of the MOW plume by a few hundred meters with
311 respect to the HadCM3 *control*. It also produces an increase in salt export that more closely

312 matches (though overshoots) observational values. However, the resulting Mediterranean-
313 Atlantic exchange is over three-times too strong compared to observational data, reorganizing
314 shallow-intermediate water circulation in the North Atlantic with significant regional climate
315 repercussions (up to +11 °C and – 7.5 °C) (Ivanovic et al. 2013). Thus, even though the
316 MOW plume in the HadCM3 *control* is around 200 m too deep and 0.9 psu too fresh, this set
317 up still reaches the best compromise to date for achieving a realistic strength of exchange.
318 Ivanovic et al. (2013) discuss this in more detail and propose ways in which the disparity
319 between MOW plume depth, flow strength and salt export could be overcome in the future.

320

321 **2.3. Experiment design**

322 To test the sensitivity of modern climate to the presence, strength and salinity of
323 Mediterranean-Atlantic water exchange, we performed three HadCM3 experiments. The
324 simulations represent extremes compared to modern Mediterranean conditions, but are well
325 within the geologic constraints of events such as the Messinian Salinity Crisis (5.96-5.33
326 Ma), eustatic sea level changes and Mediterranean sapropel formation (e.g. Clauzon et al.
327 1996; Fleming et al. 1998; Béthoux and Pierre 1999; Milne et al. 2005; Flecker and Ellam
328 2006; Marino et al. 2007; Roveri et al. 2008; Rohling et al. 2008; Govers et al. 2009; de
329 Lange and Krijgsman 2010; Osborne et al. 2010). These are idealised experiments, and
330 although they are not set-up to be specifically realistic in a geologic, modern, or future
331 context, they directly test extreme cases of Mediterranean variability. Thus, these
332 experiments provide a robust platform from which to interpret further ‘realistic’ simulations
333 of changes to Mediterranean-Atlantic exchange and the Mediterranean hydrological balance:

334 (a) The first experiment is a pair of simulations designed to examine how the presence of
335 Mediterranean-Atlantic exchange affects North Atlantic circulation and climate in
336 HadCM3. It consists of *no-exch*, in which we have turned off the HadCM3

337 Mediterranean-Atlantic pipe so that there is no exchange between the two basins, and
338 the *control*.

339 (b) In the HadCM3 *pipe* parameterisation, μ is a measure of the restriction of flow
340 between the Mediterranean and Atlantic. As such, it is a crude representation of (i) the
341 geometry of the Gibraltar Straits and (ii) the complex flow of water over the Gibraltar
342 Straits sills, including local *meddies*. Thus, the second experiment is designed to
343 examine climate-ocean sensitivity to changes in the restriction and mixing of the
344 exchange. In the ‘real world’, this could be brought about by rising/falling sea levels,
345 tectonic adjustment of the Straits, or changes in Mediterranean circulation. The
346 experiment comprises five simulations, each with different strengths (or restrictions)
347 of exchange for a given temperature and salinity gradient across the Gibraltar Straits:
348 *quart-exch*, *half-exch*, *control*, *doub-exch* and *quad-exch*, which have exchange
349 coefficients that are equal to $0.25\mu_c$, $0.5\mu_c$, μ_c , $2\mu_c$ and $4\mu_c$, respectively, where μ_c is
350 the standard (*control*) coefficient of mixing for the temperature/salinity gradient
351 driven Mediterranean-Atlantic exchange.

352 (c) The experiment is made up of three simulations: *fresh-Med*, *control* and *salt-Med*. For
353 *fresh-Med* and *salt-Med*, we have forced the entire Mediterranean basin, but nowhere
354 else, to have a constant salinity of 19 psu (approximately half the *control* salinity) and
355 76 psu (approximately double the *control* salinity) respectively, at every timestep for
356 the duration of the model run. This means that salt is not conserved and the
357 simulations do not directly represent ‘real world’ scenarios. However, in this
358 experiment, the volume integral for the global ocean changes by only ~ 0.1 psu over
359 500 years. Thus, the changes are small (0.2-0.4 %) and so do not present a problematic
360 salt source/sink for understanding the physical mechanisms at work in these idealised
361 simulations.

362 For all three experiments we have made no alterations to the *control*, using the standard
363 HadCM3 modern set-up described above, and have also included three conservative ocean
364 tracers with an arbitrary volume-density of 1 m^{-3} to the Mediterranean basin at the very start
365 of the run:

366 (i) Tracer 1 is the shallow water tracer and was applied to the upper 150 m of the water
367 column.

368 (ii) Tracer 2 is the intermediate water tracer and was applied to water between 150 m and
369 500 m deep.

370 (iii) Tracer 3 is the deep water tracer and was applied to depths below 500 m.

371 Thus, as the tracer-spiked water exchanges with the Atlantic, we are able to directly track the
372 pathways of MOW and monitor the slow spread and mixing of Mediterranean water in the
373 global ocean through time.

374 All simulations were run for 500 years using a pre-industrial climate and modern
375 continental configuration. They were initialised using dump files from the HadCM3 public
376 release spin-up simulation, published by Gordon et al. (2000). For all simulations, near steady
377 state was reached within the first 400 years of model run, and the climate means shown in
378 this study were calculated from the remaining 100 years.

379

380 **3. Results and Discussion**

381 In the following discussion, we present the results of our investigation into modern ocean and
382 climate sensitivity to changes in the presence, strength and salinity of Mediterranean Atlantic
383 exchange. The discourse is divided into three subsections, one for each experiment outlined
384 in section 2.3., and in that order.

385

386 **3.1. Presence of Mediterranean-Atlantic exchange**

387 The climate differences discussed in this section are given as the climate anomalies achieved
388 in *control* with respect to *no-exch*; that is, the effect of having Mediterranean-Atlantic
389 exchange (and hence MOW) in HadCM3 versus no exchange (and no MOW).

390 In *control*, MOW spreads westward from the Gibraltar Straits (35° N), between depths of
391 600 m and 2500 m, reduces net southward flow of NADW at 800-2000 m depth and weakens
392 the AMOC north of the Gibraltar Straits (35° N) by up to 2 Sv (11.1 %, Fig. 2a).
393 Interestingly, this result counters speculation by Reid (1979), Bethoux et al. (1999) and
394 Gómez (2003) that without MOW, modern NADW formation (and hence the AMOC) would
395 be weaker. In fact, South of the Gibraltar Straits (35° N), the AMOC is strengthened by up to
396 1 Sv (16.7 %; Fig. 2a). This strengthening is in good agreement with the conclusions of
397 Rahmstorf (1998) and Chan and Motoi (2003), whose GCM results suggest that the presence
398 of MOW in the North Atlantic increases the deeper, southward-bound AMOC component by
399 1-2 Sv. In our model, this reorganisation of the AMOC is due to a change in the North-South
400 density gradient along the Atlantic; the presence of MOW reduces the density gradient
401 between the sites of NADW formation and the Gibraltar Straits and increases the density
402 gradient between the Gibraltar Straits and the South Atlantic (Fig. 2b). This is why AMOC is
403 reduced north of the Straits and increased south of it.

404 Furthermore, computing the AMOC-associated freshwater transport at the southern
405 boundary of the Atlantic (F_{ov}), as done by Hawkins et al. (2011), we find that the increased
406 export of relatively salty water from MOW to the Southern Ocean in *control* enhances net
407 freshwater import by 0.03 Sv (an increase of 11 %), compared to *no-exch*. Others (incl.
408 Rahmstorf 1996; Dijkstra 2007; Huisman et al. 2010; Hawkins et al. 2011) have suggested
409 that such net freshwater import (positive F_{ov}) to the North Atlantic negatively feeds-back to
410 AMOC strength and promotes a mono-stable AMOC regime, whereas net freshwater export
411 to the Southern Ocean (negative F_{ov}) promotes bistability in the AMOC. For example, in the

412 case of positive F_{ov} , a decrease in AMOC strength would result in the accumulation of salt in
413 the North Atlantic, promoting deep mixing, increasing AMOC strength and thereby
414 stabilising NADW formation. Conversely, for a system with negative F_{ov} , AMOC weakening
415 leads to freshening in the North Atlantic, further reducing NADW formation and AMOC
416 strength, pushing it towards a weak (or even an ‘off’) mode of circulation. Thus it follows
417 that an increase in net freshwater import to the North Atlantic achieved with the presence of
418 Mediterranean-Atlantic exchange in HadCM3 acts to further stabilise the current mode of
419 AMOC, corroborating similar findings by Bigg and Wadley (2001) and Artale et al. (2002).

420 However, the respective 1-2 Sv weakening and strengthening of different AMOC
421 components that is caused by the presence of MOW in the North Atlantic (Fig. 2), has
422 negligible impact on HadCM3 climate. This is consistent with the findings of Rahmstorf
423 (1998), but contrary to those of Chan and Motoi (2003), who propose that MOW strengthens
424 Antarctic Bottom Water formation, warming Southern Ocean air temperatures by up to 6 °C.
425 We suggest that our results are an inevitable product of the strong, stable, modern AMOC,
426 which at 26.5° N has an overturning strength of 18 ± 2 Sv in HadCM3 (this study) and 18.7
427 ± 5.6 Sv in recent observations (Cunningham et al. 2007), but only 10 Sv (approx.) in the
428 control simulation performed by Chan and Motoi (2003). Perhaps the role of Mediterranean-
429 Atlantic exchange is more important for periods of weaker NADW formation or a bi-stable
430 ocean (Broecker et al. 1990; Cacho et al. 2000; Bigg and Wadley 2001; Artale et al. 2002;
431 Voelker et al. 2006; Rogerson et al. 2010; Penaud et al. 2011), but it is assuredly clear that
432 modern HadCM3 climates are insensitive to the presence of Mediterranean-Atlantic
433 exchange, despite the MOW-induced saline and thermal anomalies produced in intermediate
434 to deep North Atlantic waters.

435

436 **3.2. Strength of Mediterranean-Atlantic exchange**

437 The exchange of water through the Gibraltar Straits governs the temperature and salinity
438 characteristics of the Mediterranean Sea and, to a lesser extent, the North Atlantic Ocean.
439 These in turn control the temperature/salinity gradients across the Straits, as well as affecting
440 large-scale ocean circulation in the two basins, negatively feeding back to regulate the initial
441 change (Candela 1991; Bethoux and Gentili 1999; Mariotti et al. 2002; Rogerson et al. 2011;
442 Sanchez-Gomez et al. 2011). Thus, the effect of changing the coefficient of Mediterranean-
443 Atlantic exchange in HadCM3 is not straightforward. As explained in section 2.2, although
444 there is no advection of water through the *pipe*, the exchange in temperature and salinity
445 induces flow in and out of boxes on either side of the *pipe*. What we call the flux of water
446 transported through the Gibraltar Straits, is the flux calculated in the westernmost grid boxes
447 of the Straits, immediately adjacent to the Morocco-Spain land bridge.

448 For the simulations with a lower coefficient of exchange than the *control* (*quart-exch* and
449 *half-exch*), the flux of water transported through the Gibraltar Straits is initially 0.3 Sv,
450 compared to 1 Sv in *control*. Because of this reduced mixing between the Mediterranean and
451 the Atlantic, the Alboran Sea in the Mediterranean becomes accumulatively saltier (on
452 average, +1.85 psu for *half-exch* and +2.40 psu for *quart-exch* by the end of the run), whilst
453 the Gulf of Cadiz in the North Atlantic becomes accumulatively fresher (on average, -0.05
454 psu for *half-exch* and -0.15 psu for *quart-exch* by the end of the run). The resulting increase
455 in temperature/salinity gradients across the Straits then counteracts the reduced mixing
456 coefficients used in *quart-exch* and *half-exch*, elevating Mediterranean-Atlantic exchange
457 from its initial state. Thus, as the temperature/salinity gradients become steeper through the
458 run, so the flow across the Gibraltar Straits increases back towards the *control* state (Fig. 3)
459 and vice versa for an increased coefficient of mixing. This ‘relaxation’ towards an
460 equilibrium state is not unique to the four perturbed mixing coefficient simulations. We also
461 observe similar behaviour in *control* (Fig. 3), reaching a steady state exchange of 1 Sv after

462 approximately 100 years of model run. For *quart-exch*, the transport flux reaches a steady
463 state centred at 0.65 Sv after around 200 years of model run (Fig. 3) and *half-exch* recovers to
464 a steady state flow of around 0.8 Sv in about half that time (~ 100 years). This negative
465 feedback to flow strength indicates the strong influence of temperature/salinity gradients
466 across the Straits in governing the intensity of exchange and an element of insensitivity to
467 changes in the coefficient of mixing. Notably, the 0.8 Sv of exchange reached by *half-exch*
468 after 100 years of model run, more closely matches observations of $\sim 0.74 \pm 0.05$ Sv (e.g.
469 García-Lafuente et al. 2011) than the 1 Sv achieved by *control*. However, the Mediterranean
470 salt export of 0.15 psu Sv for *half-exch* is much less realistic than the already relatively low
471 levels of export in *control*; 0.6 Sv compared to the observed ~ 1.5 psu Sv (Bryden et al.
472 1994).

473 The immediate effect of increasing the coefficients of exchange in *doub-exch* and *quad-*
474 *exch* is to increase the transport of water across the Gibraltar Straits by up to around 0.6 Sv
475 for *doub-exch* and by up to around 2.4 Sv for *quad-exch*, with respect to the 1 Sv of flow
476 achieved with the *control* (Fig. 3). However, by the same feedback-processes that reduced the
477 effect of decreasing the coefficient of exchange, this initial strengthening progressively
478 reduces towards *control* values. Still, by the end of the run, the Alboran Sea in the Western
479 Mediterranean has, on average, freshened by 2.30 psu in *doub-exch* and by 3.75 psu in *quad-*
480 *exch*, due to enhanced Atlantic inflow. Similarly, due to greater Mediterranean outflow to the
481 Atlantic, average ocean salinity in the vicinity of the Gulf of Cadiz has increased by 0.05 psu
482 in both *doub-exch* and *quad-exch*. As a result, Mediterranean-Atlantic exchange in *doub-exch*
483 and *quad-exch* generally remains higher than *control* (Fig. 3). After approximately 150 years
484 of model run, *doub-exch* reaches a steady state Mediterranean-Atlantic exchange of 1.3 Sv.
485 *Quad-exch*, on the other hand, takes almost 200 years to settle with a flow of 1.6 Sv across
486 the Gibraltar Straits (Fig. 3). Although the enhanced Mediterranean-Atlantic exchanges in

487 *doub-exch* and *quad-exch* settle at almost twice the strength of observed values, the levels of
488 salt export to the Atlantic (0.9 psu Sv in *doub-exh* and 1.0 psu Sv in *quad-exch*) are more
489 realistic than the 0.6 psu Sv exported in *control*.

490 However, in HadCM3, these changes in flow strength (and salt export) through the
491 Gibraltar Straits have negligible impact on Atlantic circulation and climate, although they do
492 influence AMOC stability. With respect to there being no exchange between the
493 Mediterranean and the Atlantic (*no-exch*), F_{ov} increases by 0.01 Sv (3.7 %) for *quart-exch*,
494 and thereafter increases in increments of 0.01 Sv per doubling of the mixing coefficient for
495 *half-exch*, *control*, *doub-exch* and *quad-exch*. Thus, for *quad-exch*, F_{ov} is 0.05 Sv (18.5 %)
496 greater than for *no-exch*, and 0.02 Sv (6.7 %) greater than for *control*. This further supports
497 the proposition that Mediterranean-Atlantic exchange acts to stabilise the current AMOC
498 mode, as discussed in section 3.1., and shows that even a quadrupling of the coefficient of
499 exchange across the Gibraltar Straits is insufficient to increase the sensitivity of HadCM3
500 climate to the presence of Mediterranean-Atlantic exchange.

501 Nevertheless, we do not rule out the possibility that Atlantic circulation and climate are
502 affected by changes in Mediterranean-Atlantic exchange intensity. Mediterranean Outflow
503 Water (MOW) in *quart-exch*, *half-exch*, *doub-exch* and *quad-exch* remains centred at 1200-
504 1500 m, as it does in the *control*, and so the perturbations in exchange intensity only impact
505 deeper Atlantic waters. The very presence of MOW at these deeper layers is enough to
506 enhance F_{ov} , suggesting that it acts to stabilise AMOC, but nothing more. We therefore
507 consider that in HadCM3, MOW is some 200-300 m deeper than the plume observed in the
508 modern Atlantic Ocean (Boyer et al. 2009). Should MOW shoal, then changes in
509 Mediterranean-Atlantic flow strength would influence shallower, intermediate North Atlantic
510 currents, and so could significantly impact high northern latitude climates (Ivanovic et al.
511 2013). As the salinity of the Mediterranean directly affects the salinity and hence buoyancy

512 of MOW in the Atlantic (e.g. Bethoux and Gentili 1999; Mariotti et al. 2002; Rogerson et al.
513 2011), we propose that changing Mediterranean salinity has a greater impact on Atlantic
514 circulation and global climate than changing the coefficient of mixing across the Gibraltar
515 Straits. Thus, in the following section we investigate the impact of having a fresher (*fresh-*
516 *Med*) and a saltier (*salt-Med*) Mediterranean in HadCM3.

517

518 **3.3. Mediterranean salinity**

519 As discussed in section 2.2., and as illustrated by the damped effect of changes in mixing
520 coefficients across the Gibraltar Straits (section 3.2.), the temperature/salinity gradients
521 between the westernmost Alboran Sea and easternmost Gulf of Cadiz is the primary control
522 for Mediterranean-Atlantic flow-strength in HadCM3. Therefore, it is unsurprising that
523 halving (*fresh-Med*) and doubling (*salt-Med*) Mediterranean salinity has a dramatic impact on
524 flow strength across the Gibraltar Straits in the *pipe*. In *fresh-Med*, there is a three-fold
525 strengthening of Mediterranean-Atlantic exchange, settling at 3.0 Sv of flow in both
526 directions (almost double that achieved by *quad-exch*, Fig. 3), and the effect is even stronger
527 in *salt-Med*, reaching 5.3 Sv at the end of the run (over three-times that achieved by *quad-*
528 *exch*). Also, unlike *quart-exch*, *half-exch*, *doub-exch* and *quad-exch*, there is barely any
529 relaxation of flow strength in the centuries following the initial ramp-up. This is because
530 Mediterranean salinity is held constant throughout the simulations, which impedes the
531 negative feedback of enhanced mixing reducing the temperature/salinity gradients.

532 The forced increase in Mediterranean salinity to 76 psu in *salt-Med* enforces the two-layer
533 Mediterranean-Atlantic exchange structure already in place for *control*, whereas the
534 freshening to 19 psu in *fresh-Med* completely reverses this structure. As a result *salt-Med* and
535 *fresh-Med* have different effects on North Atlantic Ocean circulation, and so will be
536 discussed separately below.

537

538 **3.3.1. Halving Mediterranean salinity**

539 In the modern ocean, western Mediterranean salinity is on average ~ 38 psu. For *fresh-Med*,
540 we forced Mediterranean salinity to be a constant 19 psu across the whole basin and for the
541 duration of the run. This reverses the salinity gradient across the Gibraltar Straits, causing net
542 salt import to the Mediterranean of 3.35 psu Sv, compared to net export of 0.6 psu Sv in
543 *control*. The Atlantic is now 17 psu saltier, and hence denser, than the Mediterranean, which
544 forces Atlantic water to contribute the lower ~ 500 m of flow between the two basins, with
545 MOW occupying the upper ~ 500 m of exchange in the *pipe*. This shoals the MOW plume to
546 the surface of the North Atlantic and as a result, it takes a different flow-path (Fig. 4). Thus,
547 in *fresh-Med*, MOW is routed northward along the Atlantic's eastern boundary, bypassing the
548 North Atlantic subtropical gyre to contribute directly to the more northerly, adjacent subpolar
549 gyre. Consequently, the subpolar gyre is both widened, stretching a further 10° S and 10° E in
550 the North Atlantic, and strengthened, by up to 4 Sv, compared to *control*. This increases the
551 provision of relatively warm, shallow, more southerly sourced waters to the Greenland-
552 Iceland-Norwegian (GIN) Seas, raising their sea surface temperatures by up to 2.5 °C (Fig.
553 5). Combined with subsequent heat-release to the overlying atmosphere, this causes a decline
554 in sea ice coverage over these high latitude sites, reducing surface albedo and amplifying the
555 initial warming. With respect to *control*, annual mean surface air temperatures over the GIN
556 Seas have warmed by up to 1.8 °C (Fig. 6b) by the end of the run and annual mean sea ice
557 concentration has declined by up to 10 %; up to +2.7 °C and -15 % respectively in the boreal
558 winter and spring, when the GIN Seas temperature and sea ice anomalies are greatest.

559 Moving focus to the North West Atlantic, the stronger, wider subpolar gyre promotes
560 exchange between the Labrador Sea and the North Atlantic. As a result, there is an increase in
561 flow of relatively cool and fresh, high latitude waters (from the GIN Seas) counter-clockwise

562 into the Labrador Sea, cooling the overlying atmosphere of the southern Labrador Sea (Fig.
563 6b). This enhanced circulation also boosts the south-easterly expulsion of relatively cool and
564 fresh water from the Labrador Sea, exaggerating the cold-tongue protruding into the North
565 Atlantic, centred at a depth of 40-100 m (Fig. 7). Furthermore, the south-eastward extension
566 of the subpolar gyre limits northward flow of relatively warm, low latitude water to the
567 central North Atlantic 40-50° N. This, combined with the increased injection of colder water
568 from high latitudes (the GIN and Labrador Seas) cools the North Atlantic water column by up
569 to 4.5 °C (Fig. 7), with respect to *control*. The effect is greatest where these processes
570 coalesce, centred around 45° N and 39° W (Figures 6b and 7), and as a result, the overlying
571 atmosphere cools by up to 2.5 °C (annual mean), leading to a very localised increase in
572 annual mean precipitation-evaporation of up to 76 %, which is equivalent to wetting of up to
573 1 mm day⁻¹.

574 In the northernmost North Atlantic, vertical density-stratification in the upper 650 m is
575 increased by the compounded effect of mixing with the relatively fresh MOW and the
576 boosted southward contribution of relatively fresh, shallow to intermediate water from the
577 GIN Seas. In both *fresh-Med* and *control*, the core of the AMOC lies at around 800 m depth.
578 Consequently, diminished vertical mixing in the upper 650 m of the water column reduces
579 NADW formation and weakens the AMOC by up to 4 Sv (Fig. 8b). As a result, F_{ov} in *fresh-*
580 *Med* decreases by 0.1 Sv (33 %), compared to *control*. Now at only 0.2 Sv, this reduced
581 freshwater import suggests that not only is AMOC weaker, but that it is closer to reaching a
582 point of bistability (e.g. Hawkins et al. 2011). Also, compared to *control*, the reduced *fresh-*
583 *Med* AMOC transfers less heat polewards from the equator, which further enhances cooling
584 in the shallow to intermediate North Atlantic water column.

585 Returning to the immediate vicinity of the Gibraltar Straits, freshening the Mediterranean
586 to 19 psu reduces North Atlantic salinity throughout the water column (Fig. 9a). This is by

587 the dual effect of (i) having a fresher, shallow MOW that decreases salinity in the upper
588 North Atlantic and (ii) removing the deeper, relatively saline MOW plume that is present in
589 *control*. As a result, vertical stratification increases (Fig. 9c) and vertical mixing is reduced.
590 Furthermore, because Mediterranean salinity is held constant (at 19 psu), the Mediterranean
591 basin also becomes highly stratified, with almost no vertical mixing taking place. This
592 restricts warmer surface waters to the upper 15 m, causing the deeper Mediterranean to cool
593 by up to 6 °C. As MOW is predominantly formed from deep Mediterranean water both in the
594 model (Fig. 4) and the modern ocean (Cacho et al. 2000; Gómez 2003; Voelker et al. 2006),
595 this cools the MOW plume in *fresh-Med* with respect to *control*. Thus, in the easternmost
596 North Atlantic, a shoaled, relatively cold MOW plume replaces the deeper, relatively warm
597 plume in *control*, cooling and freshening the entire water column, and increasing vertical
598 stratification (Fig. 9). This cools the overlying atmosphere by up to 4 °C (Fig. 6b), following
599 the south-westerly track of the shallow, relatively fresh, cool MOW plume (Fig. 4b).

600

601 **3.3.2. Doubling Mediterranean salinity**

602 For *salt-Med*, we forced Mediterranean salinity to be approximately double (76 psu) the
603 modern average, for the duration of the run. This substantially increased the
604 temperature/salinity gradients across the Gibraltar Straits (similar to *fresh-Med*, but opposite
605 in direction) and so enhanced Mediterranean-Atlantic exchange by 4.3 Sv at the end of the
606 run, with respect to *control*. As a result, there is a fifteen-fold increase in Mediterranean salt
607 export to the North Atlantic in *salt-Med* compared to *control*, settling around 8.9 psu Sv by
608 the end of the run and raising Atlantic salinity in the intermediate and deep layers. Despite
609 the opposite change from *control* in *salt-Med* compared to *fresh-Med*, and their opposite
610 effects on flow through the Gibraltar Straits and North Atlantic salinity, the trends in climate
611 anomalies achieved in both simulations are notably similar, especially in the GIN Seas region

612 (Fig. 6). However, any similarities in climate signal are misleading; the *salt-Med* climate
613 anomalies are brought about through different mechanisms than the *fresh-Med* anomalies are.

614 Due to enhanced Mediterranean-Atlantic exchange, the stronger, denser, MOW plume
615 spreads further and deeper in the North Atlantic and there is a stronger, shallow flow of water
616 across the Atlantic into the Mediterranean. This boosts both the southward spread of deep,
617 saline waters in the North Atlantic (Fig. 10) and the northward draw of shallow, tropical
618 waters. As a result, the AMOC is strengthened by up to 3 Sv south of the MOW injection
619 (35° N, Fig. 8c) and F_{ov} by 0.2 Sv (66 %), suggesting an enhancement of the stability of the
620 AMOC. The increased export of relatively dense water to the Southern Ocean also promotes
621 Antarctic Bottom Water Formation, which strengthens by up to 5 Sv (Fig. 8c). Unlike for
622 Chan and Motoi (2003), this does not impact Southern Hemisphere sea surface temperatures
623 or atmospheric climate, but given the depth at which Antarctic Bottom Water formation
624 occurs (below 2500 m in HadCM3), this is not surprising.

625 Another effect of the increased exchange is to enhance the northward spread of relatively
626 warm, saline Mediterranean-origin waters, from around 1000 m deep and below (Fig. 11).
627 This reduces AMOC circulation North of the Gibraltar Straits (35° N) and, combined with the
628 decrease in poleward transport of shallow waters (induced by the strong eastward draw of
629 water into the Mediterranean, which weakens the Gulf Stream and North Atlantic Drift),
630 reduces NADW formation by up to 4 Sv (Fig. 8c). Furthermore, where this relatively warm,
631 salty water upwells at around 47° N 46° W, annual mean ocean temperatures and salinities
632 increase throughout the overlying water column (Fig. 12a), reducing density gradients in the
633 intermediate layers and warming the upper 200 m by up to 5.3° C. The subsequent increase in
634 heat release warms the overlying atmosphere by up to 1.1° C (annual mean, Fig. 6c), with
635 respect to *control*. In the north-easternmost North Atlantic, intermediate to deep MOW-
636 warmed waters rise over the Greenland-Scotland Ridge to flow into the interior of the GIN

637 Seas, increasing shallow water salinity and vertical mixing, and warming the upper 400 m by
638 up to 2.5 °C by the end of the run (Fig. 12b). This reduces sea ice formation in the region,
639 and increases heat exchange with the atmosphere. Additionally, the local decrease in sea ice
640 cover reduces surface albedo, positively feeding back to the initial surface warming to
641 amplify the effect. As a result, *salt-Med* reaches a steady state annual mean loss in sea cover
642 of up to 30 % and surface air warming of up to 5.1 °C (Fig. 6c). These anomalies are
643 heightened in the boreal winter and spring, reaching up to -50 % and +10.0 °C respectively.

644 It is important to point out that particularly in *salt-Med*, the depth coordinate scheme
645 employed by HadCM3 could result in a rather more diffuse spread of the highly saline MOW
646 than is physically realistic (e.g. Griffies et al. 2000). In this case, the modelled MOW plume
647 may be more interactive with Atlantic Intermediate and Deep Water than it should be, and the
648 effect on AMOC and Antarctic Bottom Waters could be biased in this respect. However, it is
649 difficult to be sure of this, given also the reduced turbulent mixing that occurs in the
650 modelled vicinity of the Gulf of Cadiz compared to the real ocean.

651 Returning our focus to the shallow ocean, the strong draw of North Atlantic water through
652 the upper 500 m of the Gibraltar Straits *pipe* increases eastward- and, to a lesser extent,
653 southward-flow across the Atlantic into the Mediterranean, as discussed above. This
654 constricts the subpolar gyre northwards and westwards, reducing the circulation of relatively
655 warm, subtropical water to higher latitudes. Consequently, the northernmost North Atlantic
656 and the Labrador Sea freshen by up to 1 psu and cool by up to 3.5 °C (both annual means),
657 also becoming more stratified in the upper 200 m (Figures 12c and 12d) with reduced vertical
658 mixing. Similar to the GIN Seas, but opposite in direction, the resulting increase in sea ice
659 cover and associated albedo feedback enhances this effect, which is greatest in the Labrador
660 Sea (Fig. 6c). By the end of the run, Labrador Sea annual mean sea ice cover has increased by
661 up to 25 % and annual mean surface air temperatures have cooled by up to 3.5 °C (Fig. 6c).

662 Again, these climate anomalies are greatest in the boreal winter and spring, when sea ice
663 cover reaches +60 % and surface air temperatures plummet by up to 8.25 °C in the Labrador
664 Sea, with respect to *control*.

665

666 **4. Summary and conclusions**

667 In HadCM3, the presence of Mediterranean-Atlantic exchange acts to strengthen the export
668 of North Atlantic waters at a depth of 1500 m to 2500 m to the Southern Ocean by up to 1 Sv,
669 in good agreement with Rahmstorf (1998) and Chan and Motoi (2003). At the same time,
670 NADW formation between 35° N and 58° N is weakened by 1-2 Sv, contrary to the
671 suggestions of Reid (1979), Rahmstorf (1998), Bethoux et al. (1999) and Gómez (2003).
672 Respectively, these changes are caused by the south- and north-westward spread of
673 Mediterranean Outflow Water (MOW) 1200-1500 m deep from 35° N. The net effect is an 11
674 % increase in F_{ov} , which may have a stabilising effect on the current AMOC regime
675 (Rahmstorf 1998; Dijkstra 2007; Huisman et al. 2010; Hawkins et al. 2011). However, these
676 small perturbations in AMOC strength are insufficient to affect the HadCM3 present-day
677 surface climate. Similarly, neither a quadrupling nor a quartering of the Mediterranean-
678 Atlantic mixing coefficient impacts North Atlantic circulation enough to induce a climate
679 signal in the surface ocean or atmosphere, although they do increase and reduce F_{ov} , and
680 hence possibly AMOC stability, respectively.

681 The only statistically significant surface climate signals arise from a change in
682 Mediterranean salinity (>95 % confidence, using student t-test). Raising (lowering)
683 Mediterranean salinity by an approximate factor of two increases (decreases) MOW salinity,
684 and hence affects the buoyancy of MOW in the North Atlantic. It also enhances (reverses) the
685 two-way Mediterranean-Atlantic flow structure by amplifying (and reversing) the salinity
686 gradient across the Gibraltar Straits. This not only affects AMOC strength and the pattern of

687 NADW formation, but is even more influential on shallow- and intermediate-water
688 circulation in the North Atlantic, impacting the subtropical and subpolar gyres, as well as
689 upwelling in the central North Atlantic and over the Greenland-Scotland Ridge. The GIN
690 Seas, the Labrador Sea, the north and central North Atlantic, and the region immediately
691 south-west of the Gibraltar Straits are most sensitive to the resulting changes in North
692 Atlantic salinity and circulation, achieving regional climate anomalies in annual mean surface
693 air temperature of ± 4 °C or more.

694 Although the changes in Mediterranean salinity in *fresh-Med* and *salt-Med* may be
695 considered extreme in a modern context (Rahmstorf 1998; Somot et al. 2006; García-Ruiz et
696 al. 2011), they are well within proxy-reconstructed fluctuations for the Mediterranean in the
697 geological past (e.g. Clauzon et al. 1996; Krijgsman et al. 1999; Flecker and Ellam 2006;
698 Rohling et al. 2008; Roveri et al. 2008; Govers et al. 2009; de Lange and Krijgsman 2010).
699 Furthermore, recent modelling work identifies the Mediterranean as being particularly
700 vulnerable to future climate trends (Mariotti et al. 2002; Gao and Giorgi 2008; Dubois et al.
701 2011; Sanchez-Gomez et al. 2011), suggesting that current climate models under-project 21st
702 Century changes in Mediterranean salinity and temperature. Also, on a much longer
703 timescale, ongoing tectonic restriction of the Gibraltar Straits may eventually culminate in a
704 salinity crisis akin to that of the Late Miocene, 5.96-5.33 Mya (Krijgsman et al. 1999).

705 However, these suppositions aside, this work shows that the presence of MOW in the
706 North Atlantic acts to enhance F_{ov} , suggesting that it also stabilises AMOC (Rahmstorf 1996;
707 Dijkstra 2007; Huisman et al. 2010; Hawkins et al. 2011); an effect that is amplified with
708 increasing Mediterranean-Atlantic flow strength. However, in the model, the correlation
709 between F_{ov} and MOW strength under present day conditions is weak. In support of Bigg and
710 Wadley (2001), Rogerson et al. (2006, 2010), Voelker et al. (2006), Penaud et al. (2011) and
711 others, we propose that Mediterranean-Atlantic exchange has the propensity to play a much

712 more important role in maintaining AMOC during periods of weaker NADW formation,
713 whether in the geologic past, or anthropogenic future. Furthermore, our results provide strong
714 evidence that fluctuations in Mediterranean-Atlantic water exchange have the greatest affect
715 on North Atlantic circulation and global climate when they instigate a combined change in
716 MOW buoyancy and flow strength.

717 Our findings may be influenced by the simulation of an overly diffuse MOW core in the
718 ocean interior. For example, a less diluted plume descending the continental shelf would
719 probably not interact with intermediate and deep Atlantic Ocean circulation as significantly
720 as in these simulations. On the other hand, the results may also be affected by the relatively
721 deep injection of MOW to the North Atlantic (1200-1500 m) in our *control*. A shallower
722 MOW plume that more closely matches observations could alter North Atlantic circulation
723 more significantly and thus have a greater climatic impact than our *control* does compared to
724 *no-exch*, as suggested by Ivanovic et al. (2013). Similarly, with a shoaled MOW plume in the
725 North Atlantic, it is likely that increased interaction of relatively warm, saline,
726 Mediterranean-sourced water with the northward flowing components of the AMOC and the
727 shallower North Atlantic gyres would enhance the effect of fluctuations in Mediterranean-
728 Atlantic flow strength shown here. Future work will examine this more closely.

729 In short, our atmosphere-ocean GCM results suggest that deeper ocean circulation
730 (including the AMOC and Antarctic Bottom Water formation) is sensitive to changes in
731 Mediterranean-Atlantic exchange, mainly through the provision of relatively saline water to
732 the deeper, exporting branches of the AMOC south of the Gibraltar Straits, as per Rahmstorf
733 (1998), Chan and Motoi (2003) and Kahana (2005). However, in the current regime of
734 relatively strong AMOC, it is the influence of Mediterranean-Atlantic exchange on MOW
735 buoyancy and strength that has the greatest effect on climate. By controlling the way MOW
736 interacts with shallow and intermediate circulation currents; including the North Atlantic

737 Drift, subtropical gyre and subpolar gyre; a large (factor of two) change in Mediterranean
738 salinity exerts a climate control of several degrees on shallow water and atmospheric
739 temperatures in the North Atlantic, GIN and Labrador Seas. Therefore, for projections of
740 future climate change, it will be important to consider the effect of regional climate trends
741 over the Mediterranean, as well as human-controlled changes in river flow into the basin,
742 within the global (or at least North Atlantic) context, especially if there are concurrent
743 changes in AMOC strength and stability. However, over the course of the next century, we
744 would not expect to see such large changes in Mediterranean or Gibraltar Straits conditions as
745 have been modelled here without direct, catastrophic, human interference with the
746 Mediterranean's hydrological budget; such as damming the Gibraltar Straits or enhanced
747 Mediterranean freshwater consumption. Small changes in Mediterranean salinity conditions
748 alone are unlikely to noticeably impact North Atlantic circulation or climate.

749 Moreover, we have shown that in such GCM research, careful consideration must be given
750 to the model-specific representation of Mediterranean Outflow in the North Atlantic. This is
751 because the buoyancy of MOW affects the extent to which it interacts with and contributes
752 towards shallow and intermediate North Atlantic currents, which in turn govern regional
753 surface climate.

754

755 **Acknowledgements**

756 This work was funded by the University of Bristol Centenary Scholarship and was carried out
757 using the computational facilities of the Advanced Computing Research Centre, University of
758 Bristol, <http://www.bris.ac.uk/acrc/>. Full access to the data produced by these simulations is
759 provided at <http://www.bridge.bris.ac.uk/resources/simulations>. We are grateful to two
760 anonymous reviewers for their valuable comments on the manuscript.

761

762

763 **References**

- 764 Alhammoud B, Meijer PT, Dijkstra HA (2010) Sensitivity of Mediterranean
765 thermohaline circulation to gateway depth: A model investigation. *Paleoceanography*
766 25: 20 PP. doi:201010.1029/2009PA001823
- 767 Artale V, Calmanti S, Sutera A (2002) Thermohaline circulation sensitivity to
768 intermediate-level anomalies. *Tellus A* 54: 159–174. doi:10.1034/j.1600-
769 0870.2002.01284.x
- 770 Baringer MO, Price JF (1999) A review of the physical oceanography of the
771 Mediterranean outflow. *Marine Geology* 155: 63–82. doi:10.1016/S0025-
772 3227(98)00141-8
- 773 Bethoux J., Gentili B, Morin P, Nicolas E, Pierre C, Ruiz-Pino D (1999) The
774 Mediterranean Sea: a miniature ocean for climatic and environmental studies and a
775 key for the climatic functioning of the North Atlantic. *Progress In Oceanography* 44:
776 131–146. doi:10.1016/S0079-6611(99)00023-3
- 777 Bethoux JP, Gentili B (1999) Functioning of the Mediterranean Sea: past and
778 present changes related to freshwater input and climate changes. *Journal of Marine*
779 *Systems* 20: 33–47. doi:10.1016/S0924-7963(98)00069-4
- 780 Béthoux J-P, Pierre C (1999) Mediterranean functioning and sapropel formation:
781 respective influences of climate and hydrological changes in the Atlantic and the
782 Mediterranean. *Marine Geology* 153: 29–39. doi:10.1016/S0025-3227(98)00091-7
- 783 Bigg GR, Wadley MR (2001) Millennial-scale variability in the oceans: an ocean
784 modelling view. *Journal of Quaternary Science* 16: 309–319. doi:10.1002/jqs.599
- 785 Bower AS, Le Cann B, Rossby T et al. (2002a) Directly measured mid-depth
786 circulation in the northeastern North Atlantic Ocean. *Nature* 419: 603–607.
787 doi:10.1038/nature01078
- 788 Bower AS, Serra N, Ambar I (2002b) Structure of the Mediterranean Undercurrent
789 and Mediterranean Water spreading around the southwestern Iberian Peninsula. *J.*
790 *Geophys. Res.* 107: 19 PP. doi:200210.1029/2001JC001007
- 791 Boyer TP, Antonov JI, Baranova OK et al. (2009) *World Ocean Database 2009*. S.
792 Levitus, Ed., NOAA Atlas NESDIS 66, U.S. Gov. Printing Office, Wash. D.C., 216pp.,
793 DVDs
- 794 Broecker WS, Bond G, Klas M, Bonani G, Wolfli W (1990) A salt oscillator in the
795 glacial Atlantic? 1. The concept. *Paleoceanography* 5: P. 469.
796 doi:199010.1029/PA005i004p00469
- 797 Bryden HL, Candela J, Kinder TH (1994) Exchange through the Strait of Gibraltar.
798 *Progress in Oceanography* 33: 201–248
- 799 Bryden HL, Kinder TH (1991) Steady 2-Layer Exchange through the Strait of
800 Gibraltar. *Deep-Sea Research Part A-Oceanographic Research Papers* 38: S445–
801 S463

- 802 Cacho I, Grimalt JO, Canals M (2002) Response of the Western Mediterranean Sea
803 to rapid climatic variability during the last 50,000 years: a molecular biomarker
804 approach. *Journal of Marine Systems* 33–34: 253–272. doi:10.1016/S0924-
805 7963(02)00061-1
- 806 Cacho I, Grimalt JO, Sierro FJ, Shackleton N, Canals M (2000) Evidence for
807 enhanced Mediterranean thermohaline circulation during rapid climatic coolings.
808 *Earth and Planetary Science Letters* 183: 417–429. doi:10.1016/S0012-
809 821X(00)00296-X
- 810 Candela J (1991) The Gibraltar Strait and its Role in the Dynamics of the
811 Mediterranean-Sea. *Dynamics of Atmospheres and Oceans* 15: 267–299
- 812 Cattle H, Crossley J, Drewry DJ (1995) Modelling Arctic Climate Change [and
813 Discussion]. *Philosophical Transactions: Physical Sciences and Engineering* 352:
814 201–213
- 815 Chan W-L, Motoi T (2003) Effects of Stopping the Mediterranean Outflow on the
816 Southern Polar Region. *Polar Meteorol Glaciol (Nat Inst Polar Res)* 25–35
- 817 Christensen JH, Christensen OB (2007) A summary of the PRUDENCE model
818 projections of changes in European climate by the end of this century. *Climatic*
819 *Change* 81: 7–30. doi:10.1007/s10584-006-9210-7
- 820 Clauzon G, Suc J-P, Gautier F, Berger A, Loutre M-F (1996) Alternate interpretation
821 of the Messinian salinity crisis: Controversy resolved? *Geology* 24: 363–366.
822 doi:10.1130/0091-7613(1996)024<0363:AIOTMS>2.3.CO;2
- 823 Cox PM, Betts RA, Bunton CB, Essery RLH, Rowntree PR, Smith J (1999) The
824 impact of new land surface physics on the GCM simulation of climate and climate
825 sensitivity. *Climate Dynamics* 15: 183–203. doi:10.1007/s003820050276
- 826 Cunningham SA, Kanzow T, Rayner D et al. (2007) Temporal Variability of the
827 Atlantic Meridional Overturning Circulation at 26.5°N. *Science* 317: 935–938.
828 doi:10.1126/science.1141304
- 829 Dietrich DE, Tseng Y-H, Medina R et al. (2008) Mediterranean Overflow Water
830 (MOW) simulation using a coupled multiple-grid Mediterranean Sea/North Atlantic
831 Ocean model. *J. Geophys. Res.* 113: 14 PP. doi:200810.1029/2006JC003914
- 832 Dijkstra HA (2007) Characterization of the multiple equilibria regime in a global
833 ocean model. *Tellus A* 59. Available at:
834 <http://tellusa.net/index.php/tellusa/article/view/15173>.
835 doi:10.3402/tellusa.v59i5.15173
- 836 Dubois C, Somot S, Calmanti S et al. (2011) Future projections of the surface heat
837 and water budgets of the Mediterranean Sea in an ensemble of coupled
838 atmosphere–ocean regional climate models. *Climate Dynamics*. Available at:
839 <http://www.springerlink.com/index/10.1007/s00382-011-1261-4>. doi:10.1007/s00382-
840 011-1261-4

- 841 Edwards JM, Slingo A (1996) Studies with a flexible new radiation code. I: Choosing
842 a configuration for a large-scale model. *Quarterly Journal of the Royal*
843 *Meteorological Society* 122: 689–719. doi:10.1002/qj.49712253107
- 844 Flecker R, Ellam RM (2006) Identifying Late Miocene episodes of connection and
845 isolation in the Mediterranean-Paratethyan realm using Sr isotopes. *Sedimentary*
846 *Geology* 188-189: 189–203. doi:10.1016/j.sedgeo.2006.03.005
- 847 Fleming K, Johnston P, Zwartz D, Yokoyama Y, Lambeck K, Chappell J (1998)
848 Refining the eustatic sea-level curve since the Last Glacial Maximum using far- and
849 intermediate-field sites. *Earth and Planetary Science Letters* 163: 327–342.
850 doi:10.1016/S0012-821X(98)00198-8
- 851 Gao X, Giorgi F (2008) Increased aridity in the Mediterranean region under
852 greenhouse gas forcing estimated from high resolution simulations with a regional
853 climate model. *Global and Planetary Change* 62: 195–209.
854 doi:10.1016/j.gloplacha.2008.02.002
- 855 García-Lafuente J, Sánchez-Román A, Naranjo C, Sánchez-Garrido JC (2011) The
856 very first transformation of the Mediterranean outflow in the Strait of Gibraltar. *J.*
857 *Geophys. Res.* 116: 7 PP. doi:10.1029/2011JC006967
- 858 García-Ruiz JM, López-Moreno JI, Vicente-Serrano SM, Lasanta-Martínez T,
859 Beguería S (2011) Mediterranean water resources in a global change scenario.
860 *Earth Science Reviews* 105: 121–139
- 861 Gent PR, McWilliams JC (1990) Isopycnal Mixing in Ocean Circulation Models.
862 *Journal of Physical Oceanography* 20: 150–155. doi:10.1175/1520-
863 0485(1990)020<0150:IMIOCM>2.0.CO;2
- 864 Giorgi F, Lionello P (2008) Climate change projections for the Mediterranean region.
865 *Global and Planetary Change* 63: 90–104. doi:10.1016/j.gloplacha.2007.09.005
- 866 Gómez F (2003) The role of the exchanges through the Strait of Gibraltar on the
867 budget of elements in the Western Mediterranean Sea: consequences of human-
868 induced modifications. *Marine Pollution Bulletin* 46: 685–694. doi:10.1016/S0025-
869 326X(03)00123-1
- 870 Gordon C, Cooper C, Senior CA et al. (2000) The simulation of SST, sea ice extents
871 and ocean heat transports in a version of the Hadley Centre coupled model without
872 flux adjustments. *Climate Dynamics* 16: 147–168. doi:10.1007/s003820050010
- 873 Govers R, Meijer P, Krijgsman W (2009) Regional isostatic response to Messinian
874 Salinity Crisis events. *Tectonophysics* 463: 109–129.
875 doi:10.1016/j.tecto.2008.09.026
- 876 Gregory D, Kershaw R, Inness PM (1997) Parametrization of momentum transport
877 by convection. II: Tests in single-column and general circulation models. *Quarterly*
878 *Journal of the Royal Meteorological Society* 123: 1153–1183.
879 doi:10.1002/qj.49712354103

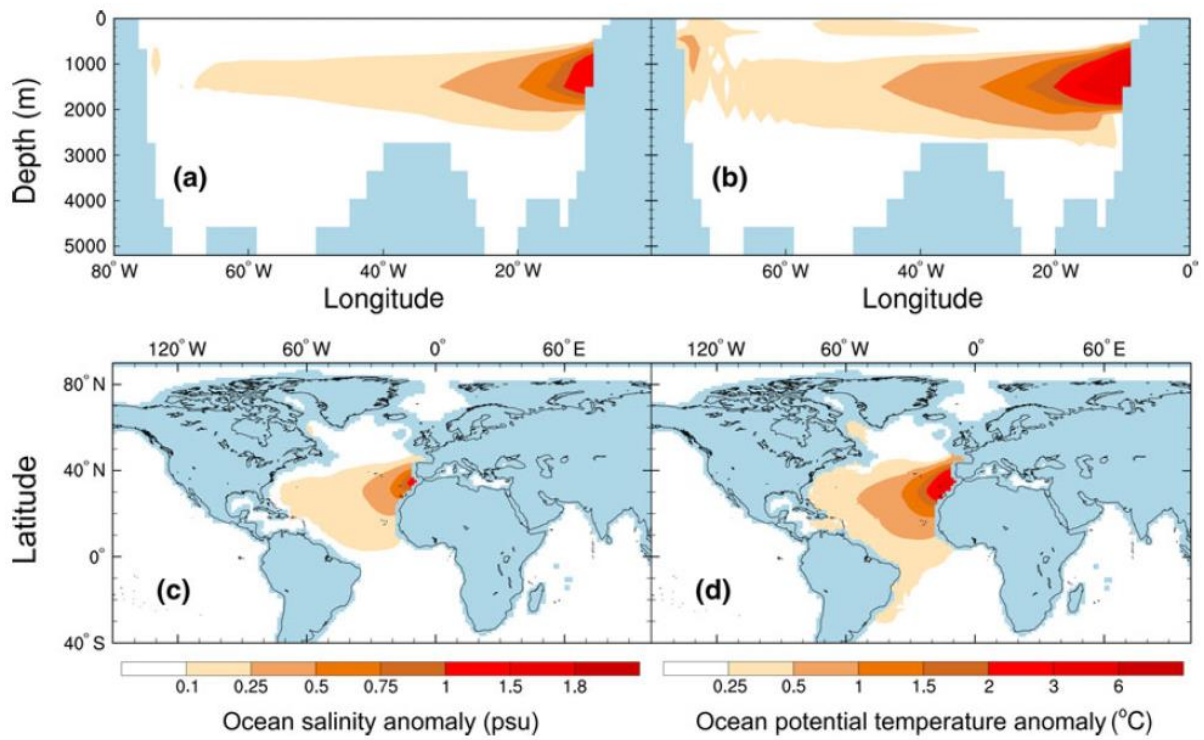
- 880 Griffies SM, Böning C, Bryan FO et al. (2000) Developments in ocean climate
881 modelling. *Ocean Modelling* 2: 123–192. doi:10.1016/S1463-5003(00)00014-7
- 882 Hawkins E, Smith RS, Allison LC et al. (2011) Bistability of the Atlantic overturning
883 circulation in a global climate model and links to ocean freshwater transport.
884 *Geophys. Res. Lett.* 38: 6 PP. doi:201110.1029/2011GL047208
- 885 Hibler WD (1979) A Dynamic Thermodynamic Sea Ice Model. *Journal of Physical*
886 *Oceanography* 9: 815–846. doi:10.1175/1520-
887 0485(1979)009<0815:ADTSIM>2.0.CO;2
- 888 Huisman SE, den Toom M, Dijkstra HA, Drijfhout S (2010) An Indicator of the
889 Multiple Equilibria Regime of the Atlantic Meridional Overturning Circulation. *Journal*
890 *of Physical Oceanography* 40: 551–567. doi:10.1175/2009JPO4215.1
- 891 Ivanovic RF, Valdes PJ, Flecker R, Gregoire LJ, Gutjahr M (2013) The
892 parameterisation of Mediterranean–Atlantic water exchange in the Hadley Centre
893 model HadCM3, and its effect on modelled North Atlantic climate. *Ocean Modelling*
894 62: 11–16. doi:10.1016/j.ocemod.2012.11.002
- 895 Johns TC, Carnell RE, Crossley JF et al. (1997) The second Hadley Centre coupled
896 ocean-atmosphere GCM: model description, spinup and validation. *Climate*
897 *Dynamics* 13: 103–134. doi:10.1007/s003820050155
- 898 Johnson J, Ambar I, Serra N, Stevens I (2002) Comparative studies of the spreading
899 of Mediterranean water through the Gulf of Cadiz. *Deep Sea Research Part II:*
900 *Topical Studies in Oceanography* 49: 4179–4193
- 901 Johnson RG (1997) Climate control required a dam at the Strait of Gibraltar. *Eos*
902 *Trans. AGU* 78: PAGE 277. doi:199710.1029/97EO00180
- 903 Jungclaus JH, Mellor GL (2000) A three-dimensional model study of the
904 Mediterranean outflow. *Journal of Marine Systems* 24: 41–66. doi:10.1016/S0924-
905 7963(99)00078-0
- 906 Kahana R (2005) Modelling the interactions between the Mediterranean and the
907 Global Thermohaline Circulations. PhD thesis, University of East Anglia, Norwich,
908 UK
- 909 Krijgsman W, Hilgen FJ, Raffi I, Sierro FJ, Wilson DS (1999) Chronology, causes
910 and progression of the Messinian salinity crisis. *Nature* 400: 652–655.
911 doi:10.1038/23231
- 912 de Lange GJ, Krijgsman W (2010) Messinian salinity crisis: A novel unifying shallow
913 gypsum/deep dolomite formation mechanism. *Marine Geology* 275: 273–277.
914 doi:10.1016/j.margeo.2010.05.003
- 915 Loget, Vandendriessche J (2006) On the origin of the Strait of Gibraltar. *Sedimentary*
916 *Geology* 188-189: 341–356. doi:10.1016/j.sedgeo.2006.03.012

- 917 Marino G, Rohling EJ, Rijpstra WIC, Sangiorgi F, Schouten S, Damsté JSS (2007)
918 Aegean Sea as Driver of Hydrographic and Ecological Changes in the Eastern
919 Mediterranean. *Geology* 35: 675–678. doi:10.1130/G23831A.1
- 920 Mariotti A (2010) Recent Changes in the Mediterranean Water Cycle: A Pathway
921 toward Long-Term Regional Hydroclimatic Change? *Journal of Climate* 23: 1513–
922 1525. doi:10.1175/2009JCLI3251.1
- 923 Mariotti A, Struglia MV, Zeng N, Lau K-M (2002) The Hydrological Cycle in the
924 Mediterranean Region and Implications for the Water Budget of the Mediterranean
925 Sea. *Journal of Climate* 15: 1674–1690. doi:10.1175/1520-
926 0442(2002)015<1674:THCITM>2.0.CO;2
- 927 Mariotti A, Zeng N, Yoon J-H et al. (2008) Mediterranean water cycle changes:
928 transition to drier 21st century conditions in observations and CMIP3 simulations.
929 *Environmental Research Letters* 3: 044001. doi:10.1088/1748-9326/3/4/044001
- 930 Mauritzen C, Morel Y, Paillet J (2001) On the influence of Mediterranean Water on
931 the Central Waters of the North Atlantic Ocean. *Deep Sea Research Part I:*
932 *Oceanographic Research Papers* 48: 347–381. doi:10.1016/S0967-0637(00)00043-1
- 933 McCartney MS, Mauritzen C (2001) On the origin of the warm inflow to the Nordic
934 Seas. *Progress in Oceanography* 51: 125–214. doi:10.1016/S0079-6611(01)00084-2
- 935 Milne GA, Long AJ, Bassett SE (2005) Modelling Holocene relative sea-level
936 observations from the Caribbean and South America. *Quaternary Science Reviews*
937 24: 1183–1202. doi:10.1016/j.quascirev.2004.10.005
- 938 New A, Barnard S, Herrmann P, Molines J-M (2001) On the origin and pathway of
939 the saline inflow to the Nordic Seas: insights from models. *Progress In*
940 *Oceanography* 48: 255–287. doi:10.1016/S0079-6611(01)00007-6
- 941 Osborne AH, Marino G, Vance D, Rohling EJ (2010) Eastern Mediterranean surface
942 water Nd during Eemian sapropel S5: monitoring northerly (mid-latitude) versus
943 southerly (sub-tropical) freshwater contributions. *Quaternary Science Reviews* 29:
944 2473–2483. doi:10.1016/j.quascirev.2010.05.015
- 945 Papadakis MP, Chassignet EP, Hallberg RW (2003) Numerical simulations of the
946 Mediterranean sea outflow: impact of the entrainment parameterization in an
947 isopycnic coordinate ocean model. *Ocean Modelling* 5: 325–356.
948 doi:10.1016/S1463-5003(02)00042-2
- 949 Penaud A, Eynaud F, Sánchez-Goñi M, Malaizé B, Turon JL, Rossignol L (2011)
950 Contrasting sea-surface responses between the western Mediterranean Sea and
951 eastern subtropical latitudes of the North Atlantic during abrupt climatic events of
952 MIS 3. *Marine Micropaleontology* 80: 1–17. doi:10.1016/j.marmicro.2011.03.002
- 953 Pope VD, Gallani ML, Rowntree PR, Stratton RA (2000) The impact of new physical
954 parametrizations in the Hadley Centre climate model: HadAM3. *Climate Dynamics*
955 16: 123–146. doi:10.1007/s003820050009

- 956 Rahmstorf S (1996) On the freshwater forcing and transport of the Atlantic
957 thermohaline circulation. *Climate Dynamics* 12: 799–811.
958 doi:10.1007/s003820050144
- 959 Rahmstorf S (1998) Influence of Mediterranean Outflow on climate. *Eos Trans. AGU*
960 79: 281. doi:199810.1029/98EO00208
- 961 Reid JL (1978) On the Middepth Circulation and Salinity Field in the North Atlantic
962 Ocean. *J. Geophys. Res.* 83: PP. 5063–5067. doi:197810.1029/JC083iC10p05063
- 963 Reid JL (1979) On the contribution of the Mediterranean Sea outflow to the
964 Norwegian-Greenland Sea. *Deep Sea Research Part A. Oceanographic Research*
965 *Papers* 26: 1199–1223. doi:10.1016/0198-0149(79)90064-5
- 966 Rogerson M, Bigg GR, Rohling EJ, Ramirez J (2011) Vertical density gradient in the
967 eastern North Atlantic during the last 30,000 years. *Climate Dynamics*.
968 doi:10.1007/s00382-011-1148-4
- 969 Rogerson M, Colmenero-Hidalgo E, Levine RC et al. (2010) Enhanced
970 Mediterranean-Atlantic exchange during Atlantic freshening phases. *Geochem.*
971 *Geophys. Geosyst.* 11: 22 PP. doi:201010.1029/2009GC002931
- 972 Rogerson M, Rohling EJ, Bigg GR, Ramirez J (2012) Paleoceanography of the
973 Atlantic-Mediterranean exchange: Overview and first quantitative assessment of
974 climatic forcing. *Rev. Geophys.* 50: 32 PP. doi:201210.1029/2011RG000376
- 975 Rogerson M, Rohling EJ, Weaver PPE (2006) Promotion of meridional overturning
976 by Mediterranean-derived salt during the last deglaciation. *Paleoceanography* 21: 8
977 PP. doi:200610.1029/2006PA001306
- 978 Rohling EJ, Schiebel R, Siddall M (2008) Controls on Messinian Lower Evaporite
979 cycles in the Mediterranean. *Earth and Planetary Science Letters* 275: 165–171.
980 doi:10.1016/j.epsl.2008.08.022
- 981 Roveri M, Lugli S, Manzi V, Schreiber BC (2008) The Messinian Sicilian stratigraphy
982 revisited: new insights for the Messinian salinity crisis. *Terra Nova* 20: 483–488.
983 doi:10.1111/j.1365-3121.2008.00842.x
- 984 Sanchez-Gomez E, Somot S, Josey SA, Dubois C, Elguindi N, Déqué M (2011)
985 Evaluation of Mediterranean Sea water and heat budgets simulated by an ensemble
986 of high resolution regional climate models. *Climate Dynamics* 37: 2067–2086.
987 doi:10.1007/s00382-011-1012-6
- 988 Serra, Ambar I, Kase R (2005) Observations and numerical modelling of the
989 Mediterranean outflow splitting and eddy generation. *Deep Sea Research Part II:*
990 *Topical Studies in Oceanography* 52: 383–408. doi:10.1016/j.dsr2.2004.05.025
- 991 Simmons AJ, Burridge DM (1981) An Energy and Angular-Momentum Conserving
992 Vertical Finite-Difference Scheme and Hybrid Vertical Coordinates. *Monthly Weather*
993 *Review* 109: 758–766. doi:10.1175/1520-0493(1981)109<0758:AEAAMC>2.0.CO;2

- 994 Skliris N, Lascaratos A (2004) Impacts of the Nile River damming on the
995 thermohaline circulation and water mass characteristics of the Mediterranean Sea.
996 *Journal of Marine Systems* 52: 121–143. doi:10.1016/j.jmarsys.2004.02.005
- 997 Somot S, Sevault F, Déqué M (2006) Transient climate change scenario simulation
998 of the Mediterranean Sea for the twenty-first century using a high-resolution ocean
999 circulation model. *Climate Dynamics* 27: 851–879. doi:10.1007/s00382-006-0167-z
- 1000 Somot S, Sevault F, Déqué M, Crépon M (2008) 21st century climate change
1001 scenario for the Mediterranean using a coupled atmosphere–ocean regional climate
1002 model. *Global and Planetary Change* 63: 112–126.
1003 doi:10.1016/j.gloplacha.2007.10.003
- 1004 Stanev EV (1992) Numerical experiment on the spreading of Mediterranean water in
1005 the North Atlantic. *Deep Sea Research Part A. Oceanographic Research Papers* 39:
1006 1747–1766. doi:10.1016/0198-0149(92)90027-Q
- 1007 Stommel H, Farmer H (1952) Abrupt Change in Width in 2-Layer Open Channel
1008 Flow. *J. Mar. Res.* 11: 205–214
- 1009 Stommel H, Farmer H (1953) Control of Salinity in an Estuary by a Transition. *J. Mar.*
1010 *Res.* 12: 13–20
- 1011 Thorpe RB, Bigg GR (2000) Modelling the sensitivity of Mediterranean Outflow to
1012 anthropogenically forced climate change. *Climate Dynamics* 16: 355–368.
1013 doi:10.1007/s003820050333
- 1014 Tsimplis MN, Bryden HL (2000) Estimation of the transports through the Strait of
1015 Gibraltar. *Deep Sea Research Part I Oceanographic Research Papers* 47: 2219–
1016 2242. doi:10.1016/S0967-0637(00)00024-8
- 1017 Vargas-Yáñez M, Zunino P, Benali A et al. (2010) How much is the western
1018 Mediterranean really warming and salting? *Journal of Geophysical Research*
1019 (Oceans) 115: 04001
- 1020 Visbeck M, Marshall J, Haine T, Spall M (1997) Specification of Eddy Transfer
1021 Coefficients in Coarse-Resolution Ocean Circulation Models*. *Journal of Physical*
1022 *Oceanography* 27: 381–402. doi:10.1175/1520-
1023 0485(1997)027<0381:SOETCI>2.0.CO;2
- 1024 Voelker AHL, Lebreiro S, Schonfeld J, Cacho I, Erlenkeuser H, Abrantes F (2006)
1025 Mediterranean outflow strengthening during northern hemisphere coolings: A salt
1026 source for the glacial Atlantic? *Earth and Planetary Science Letters* 245: 39–55.
1027 doi:10.1016/j.epsl.2006.03.014
- 1028 Xoplaki E, Luterbacher J, Gonzalez-Rouco JF (2006) Mediterranean summer
1029 temperature and winter precipitation, large scale dynamics, trends. *Il Nuovo Cimento*
1030 29: 45–54. doi:10.1393/ncc/i2005-10220-4
- 1031
- 1032

1033 **Figures**

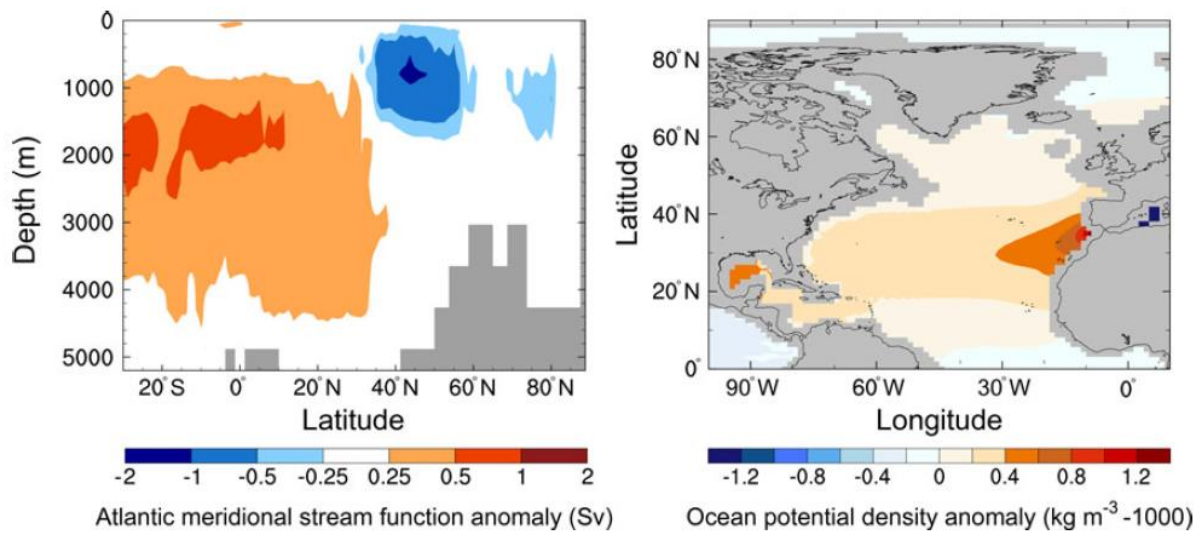


1034

1035 Figure 1. The direct effect of the presence of Mediterranean-Atlantic exchange on HadCM3
1036 Atlantic annual mean salinity and potential temperatures characteristics in HadCM3. The
1037 anomalies shown are for (a) and (c) salinity, and (b) and (d) potential temperature, as
1038 produced in *control* with respect to there being no Mediterranean Outflow Water in *no-exch.*
1039 Projections (a) and (b) are cross-sections across the North Atlantic at 35° N, which is the
1040 latitude of the Gibraltar Straits. Projections (c) and (d) are taken at an ocean depth of 1501 m.

1041

1042



1043

1044

1045

1046

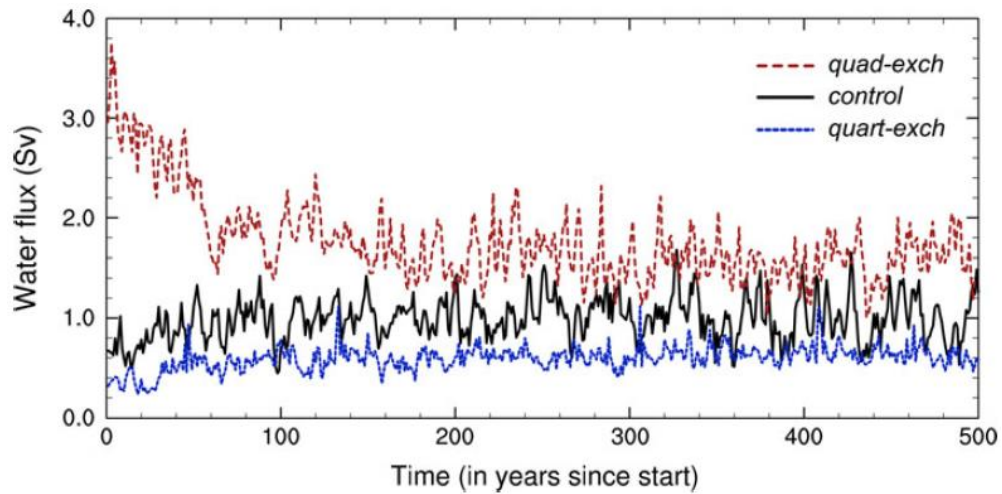
1047

1048

1049

1050

Figure 2. Annual mean anomalies for *control* with respect to *no-exch* in (a) Atlantic Meridional Overturning Circulation (as given by the stream function) and (b) North Atlantic Ocean potential density at 1501 m deep (given as the difference from 1000 kg m^{-3}). In *control* Mediterranean-Atlantic exchange occurs at 35° N . Using a student t-test, there is $>95 \%$ confidence in the significance of the anomalies shown.

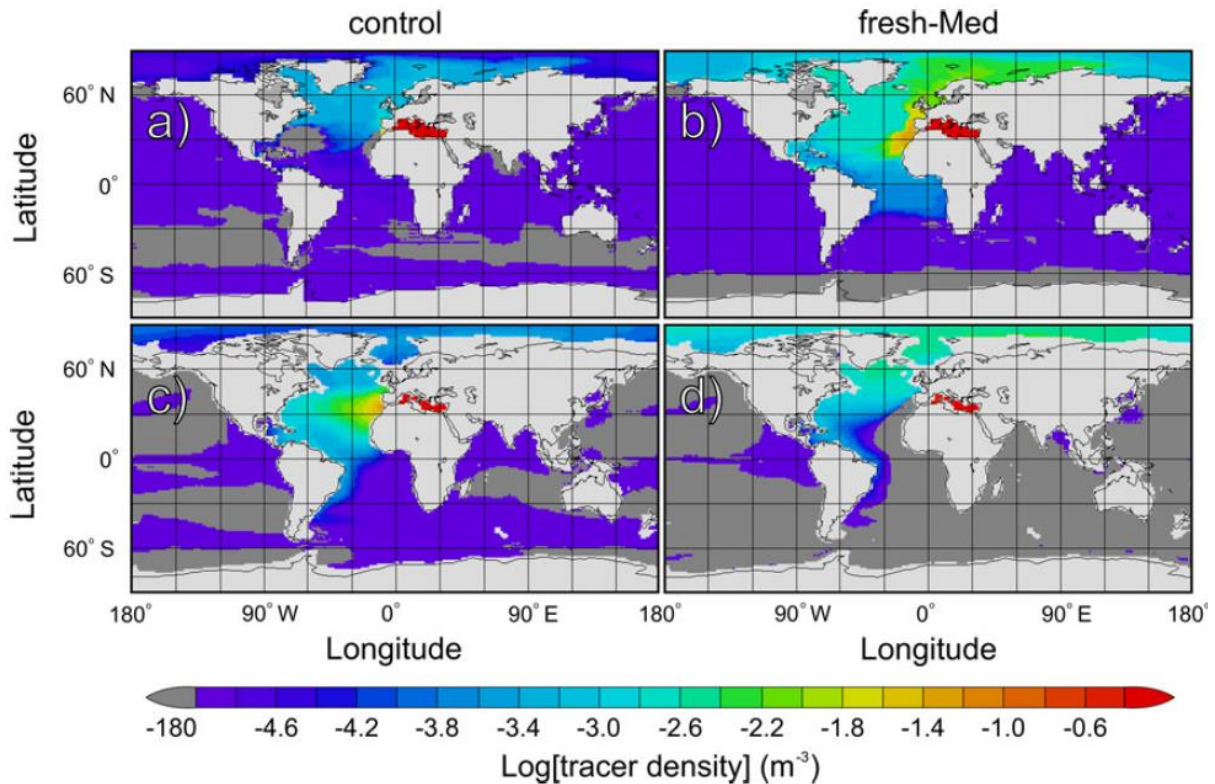


1051

1052 Figure 3. Mediterranean-Atlantic easterly and westerly water transport fluxes from the start
 1053 of each run through time for *quad-exch*, *control* and *quart-exch*. *doub-exch* and *half-exch*
 1054 show the same behaviour as *quad-exch* and *quart-exch* (respectively), but with more muted
 1055 differences from the *control*, as described in section 3.2.

1056

1057



1058

1059

1060

1061

1062

1063

1064

1065

1066

1067

1068

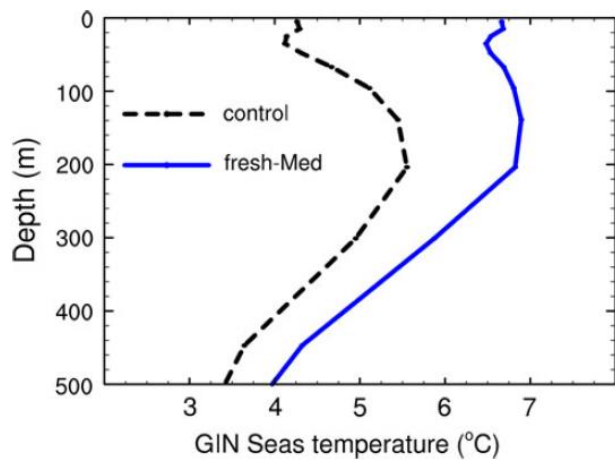
1069

1070

1071

1072

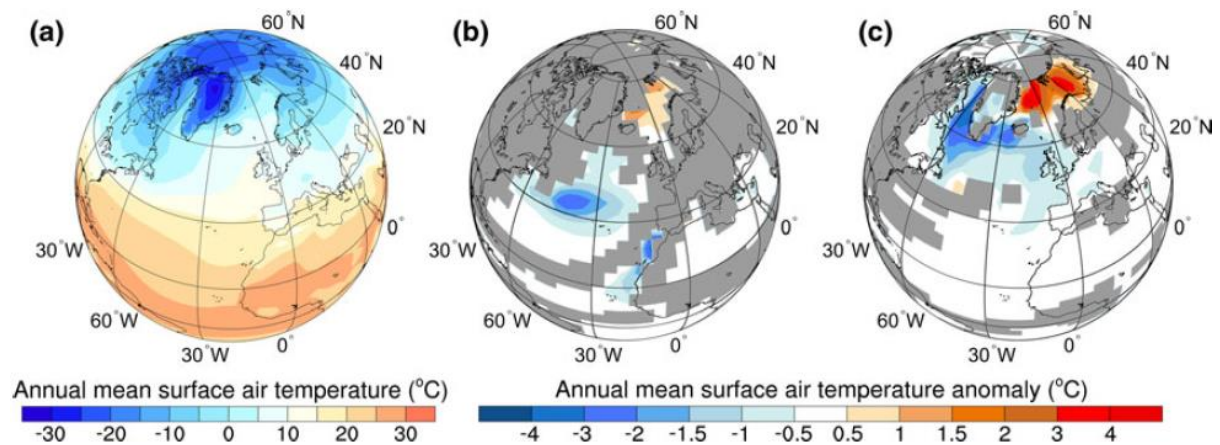
Figure 4. Log scale of the Mediterranean *deep level* tracer after 50 years of model run showing the difference between (a) and (c) *control*, and (b) and (d) *fresh-Med*. Projections (a) and (b) show the tracer at a water depth of 5 m, whereas (c) and (d) are at a depth of 1501 m. The tracer was input to the Mediterranean below 500 m deep and has an arbitrary volume density of 1 m^{-3} at the start of each simulation. After 50 years have elapsed, enough Mediterranean water has exchanged with the North Atlantic to track the flow path of Mediterranean Outflow Water (MOW) in the global ocean. An example of the deep level tracer ($>500 \text{ m}$) is illustrated because it indicates MOW's flowpath in the Atlantic. Only a very small amount of the shallow and intermediate level tracers ($<150 \text{ m}$ and $150\text{-}500 \text{ m}$, respectively; neither shown) leaves the Mediterranean; thus little information about MOW's flowpath in the Atlantic is provided by these other tracers. However, from the combined tracer results (not all shown), it is clear that most MOW consists of water originating below 500 m, even in *fresh-Med*, when MOW is a shallow current.



1073

1074 Figure 5. Greenland-Iceland-Norwegian (GIN) Seas annual mean potential temperature
 1075 through the upper 500 m of the water column at 69° N 14° W for normal *control* and *fresh-*
 1076 *Med*.

1077

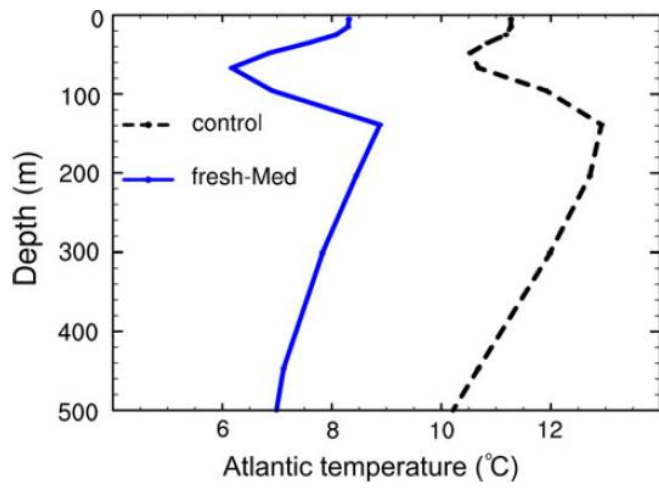


1078

1079 Figure 6. (a) Annual mean surface air temperatures produced in *control*. Annual mean surface
 1080 air temperature anomalies produced in (b) *fresh-Med* and (c) *salt-Med* with respect to *control*.
 1081 Areas with <95 % confidence in significance (using student-test) are shaded dark gray.

1082

1083



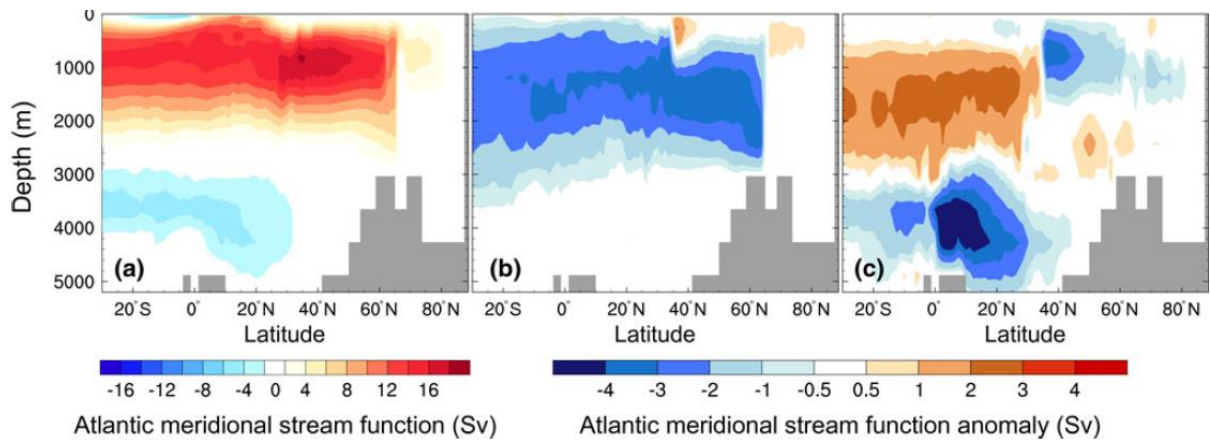
1084

1085 Figure 7. North Atlantic annual mean potential temperature through the upper 500 m of the

1086 water column at 45° N 39° W in *control* and *fresh-Med*.

1087

1088



1089

1090

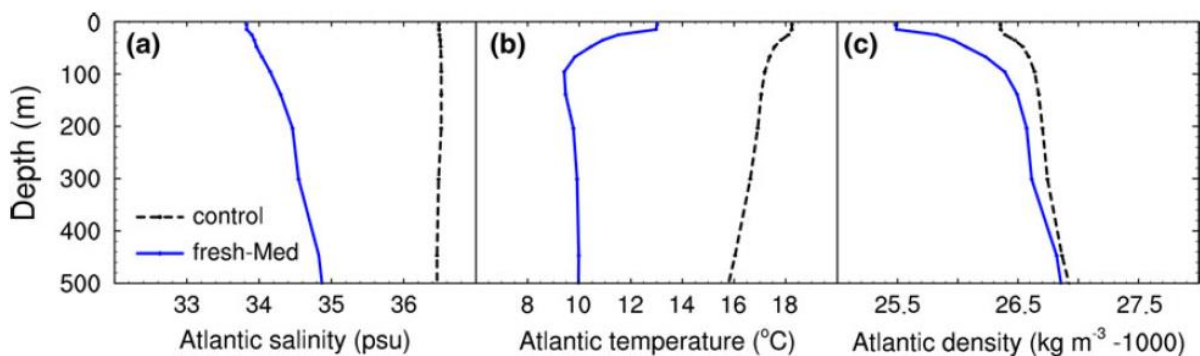
1091

1092

1093

1094

Figure 8. (a) Annual mean Atlantic Meridional Overturning Circulation (AMOC) strength in control. Annual mean AMOC strength anomalies for (b) *fresh-Med* and (c) *salt-Med*, with respect to control. Mediterranean-Atlantic exchange occurs at 35° N. The anomalies are given with >95 % confidence in their significance using a student t-test.



1095

1096

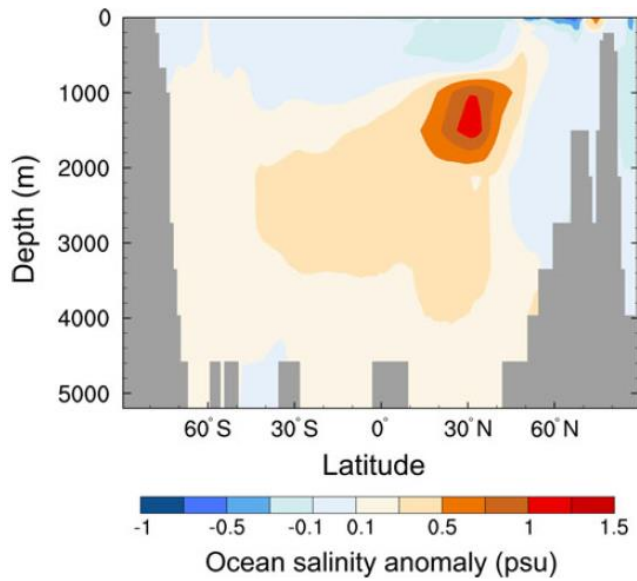
1097

1098

1099

1100

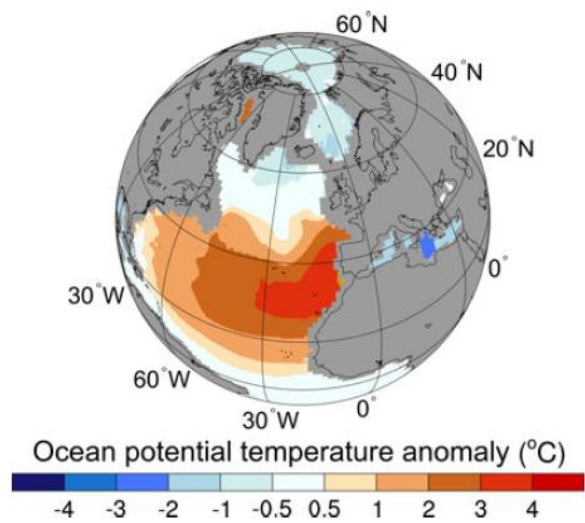
Figure 9. Eastern North Atlantic annual mean (a) salinity, (b) potential temperature and (c) potential density (given as anomalies from 1000 kg m⁻³) in the upper 500 m of the water column in control and *fresh-Med* at 33° N 10° W; the vicinity of the Gulf of Cadiz.



1101

1102 Figure 10. Annual mean salinity anomalies from North Pole to South Pole, averaged over 60°
 1103 W to 10° W to capture the Atlantic and adjoining Southern Ocean, achieved for *salt-Med*
 1104 with respect to *control*.

1105

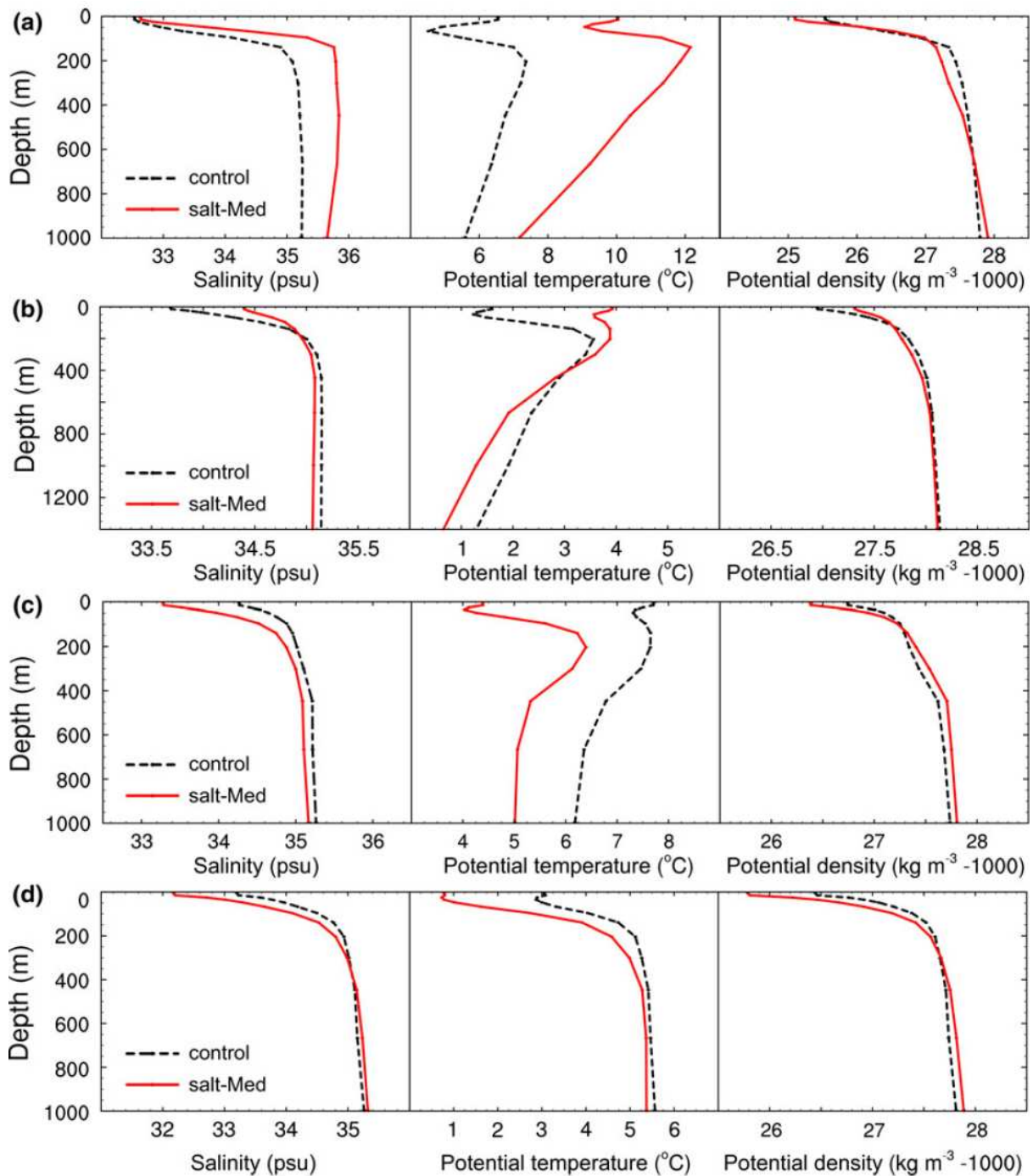


1106

1107 Figure 11. Annual mean ocean potential temperature anomalies at a depth of 1501 m for *salt-*
 1108 *Med*, with respect to *control*.

1109

1110



1111

1112

Figure 12. Ocean annual mean salinity, potential temperature and potential density (given as

1113

anomalies from 1000 kg m⁻³) in *control* and *salt-Med* at (a) 47° N, 46° W in the North

1114

Atlantic; (b) 72° N, 5° W Greenland-Iceland-Norwegian (GIN) Seas; (c) 63° N, 28° W in the

1115

northernmost North Atlantic and (d) 60° N, 60° W in the Labrador Sea.